140 AM

TECHNICAL REPORT

TECHNICAL REPORT	
Det Norske Veritas Research Report No.: 93-2018	Subject Group C1 D45 P5
Title of Report Motions of a TLP in Wind and Waves	
Client/Sponsor of project Boundary Layer Wind Tunnel Laboratory	
Work carried out by Ingunn Marton, Jan Mathisen	
Work verified by Arne Nestegård	

DET NORSKE VERITAS RESEARCH AS

DET NORSKE
VERITAS

Det Norske Veritas Research AS

ADDRESS Veritasveien 1, Høvik
POSTAL ADDRESS: P.O.Box 300, N-1322 Høvik, Norway
CABLE ADDRESS: Veritas, Oslo
TELEX: 76 192 verit n
FACSIMILE: (47) 67 57 75 20
BANKER: Den norske Bank, Acc.No. 7131.05.26821

TECHNICAL REPORT

		Date: April 23, 1993	
Det Norske Veritas Research Report No.: 93-2018	Subject Group: C1 D45 P5	Department: DNVR30	Project No.: 05480
Title of Report: Motions of a TLP in Wind and Waves		Approved by: Arne Nestegård	
Client/Sponsor of project: Boundary Layer Wind Tunnel Laboratory		Client/Sponsor ref.: -	
Work carried out by: Ingunn Marton, Jan Mathisen		Reporters sign.: Ingunn Marton Jan Mathisen	
Work verified by: Arne Nestegård		Verifiers sign.: Arne Nestegård	

Summary

Numerical simulations have been made of the surge motion time histories of a tension leg platform, under the influence of wind and wave loads. The simulation results have been compared with the results of model tests from the Boundary Layer Wind Tunnel Laboratory for different wind loads, wave loads, and the combinations. The comparison show:

Satisfactory agreement in surge natural frequency.

Satisfactory agreement in mean surge due to wind alone implying agreement in the mean wind loads.

Satisfactory agreement in the first order, wave-induced motions, excited in the frequency band of the incoming waves.

Satisfactory agreement in the mean surge due to combined wind and waves.

Fair agreement in the standard deviation of the low-frequency surge motion due to combined wind and waves, but significant differences when considering response due to wind alone or waves alone.

4 indexing terms

wind loads
drift forces
tension leg platforms
motion characteristics

Distribution statement

- ☐ No distribution without permission from the responsible department
- ☒ Limited distribution within Det Norske Veritas Research AS
- ☐ Free distribution

Date of last revision	Rev. No.		Number of pages
			43

CONTENTS

1. INTRODUCTION 1
2. NUMERICAL METHODS 2
3. EXPERIMENTS 3
4. RESPONSE IN REGULAR WAVES 5
4.1 Panel Model of TLP 5
4.2 First Order Transfer Function 6
4.3 Second Order Transfer Function 7
5. INPUT PARAMETERS FOR SIMULATION 8
5.1 Radii of Gyration 8
5.2 Restoring Forces 8
5.3 Added Mass 8
5.4 Hydrodynamic Damping 8
5.5 Aerodynamic Drag 9
5.6 Environmental Conditions 9
6. RESULTS OF TIME-DOMAIN MOTION SIMULATIONS 11
6.1 Wind Only 11
6.1 Waves Only 13
6.1 Wind and Waves 16
7. CONCLUSIONS 18
8. REFERENCES 20
APPENDIX A
APPENDIX B

1. INTRODUCTION

This report is part of a

Joint Industry Project to Study
Wind Loads and Wind/Wave Interactions on Offshore Structures:
Semi-Submersibles, Tension Leg Platforms and Compliant Towers,

organised by the Boundary Layer Wind Tunnel Laboratory, London, Ontario, and supported by the following organizations:

Amoco Production Company	ARCO Oil and Gas Company
Exxon Production Research Company	Institut Francais de Petrole
Institute for Marine Dynamics	Minerals Management Service
Mobil Research & Development Corporation	Saga Petroleum a.s.
Statoil	Det Norske Veritas Research AS

The objective originally specified for this work was: To compute motions of a semisubmersible and a tension leg platform due to wind and wave loads, comparable to the motions measured in section 4.4.6 of the proposal, "Tests in Random Sea States," and determine the uncertainties in the computed low-frequency platform motions.

Due to the limited budget available for this work, and to the large amount of time spent in interpreting the model test results, it has been necessary to exclude the semisubmersible, and only consider a limited number of cases for the tension leg platform. Furthermore, because there is considerable uncertainty in the model test results, and in the numerical modelling of the system damping, there is little reason to carry out an exhaustive comparison. These problems are addressed in some more detail in sections 2, 3, and 5.

This report compares measured surge motions of a tension leg platform model (TLP), in wind and waves, with results from computations using programs WADAM and NV1427.

The experiments were conducted at BLWT (The Boundary Wind Tunnel Laboratory) during the period 1988-90.

The comparison of the experiments with the numerical simulations is done for wave heading 0^{o}, two different sea states, and two different wind speeds. Only the surge motion is simulated which is also the largest motion for wave heading 0^{o}.

2. NUMERICAL METHODS

The potential flow calculations were carried out with the program WADAM (Ref. 1). The panel model needed for these calculations was generated using PREFEM (Ref.2). Since WADAM and PREFEM are both integral parts of the Sesam package, the transfer of the panel data between the two programs is handled automatically.

WADAM is a diffraction and Morison theory program for the analysis of the interaction of surface waves with offshore structures. It is based on a three-dimensional panel method to evaluate the velocity potentials and hydrodynamic parameters. The free-surface condition is linearized and the flow is assumed to be ideal and time harmonic.The radiation and diffraction velocity potentials on the wetted surface of the body are determined from the solution of an integral equation, obtained by using Green's theorem with the free-surface source-potential as the Green function. Transfer functions for first-order, wave-induced motions, and for second-order, mean drift forces in regular waves are computed by the program.

The simulations of the platform motions in irregular waves were carried out with the program NV1427 (Ref. 3, 12). This program computes the motion time history of the moored platform. The first-order, wave frequency motions are assumed physically independent of the low-frequency, wind and wave-drift force excited motions. However, correlation effects due to excitation from the same incident waves are included. NV1427 generates a realisation of a wind and wave time history, under stationary conditions.The first order, wave-frequency motion response of the platform to the wave time history is generated from the transfer functions. The low-frequency response to wind and second-order wave forces is computed through solution of the equations of motion in the time-domain, taking damping and tether forces into account. The wave-frequency and low-frequency motions are then superposed.

Low-frequency motions are resonant in nature, so the damping forces are essential for accurate determination of the magnitude of the motions. Only a linearised hydrodynamic damping coefficient is applied in the present analysis. The magnitude of this damping coefficient is based on results from the model tests. NV1427 also includes a facility for a viscous hydrodynamic damping term (proportional to the square of the relative velocity), but this is not used here, since the total hydrodynamic damping is based on a linear term only. Numerical methods for prediction of wave diffraction damping forces (second order potential damping forces) have become available recently, but have not been applied here either. There are indications in the model test results, showing that aerodynamic damping may be significant. Aerodynamic damping has not been included here, because there is no facility for this in NV1427 at present. It would be fairly straightforward to modify NV1427 to include such a term.

An ad hoc interface program (called ugrif) was written to convert the output results from WADAM to the input format required by NV1427.

3. EXPERIMENTS

The experiments on the TLP in wind and waves were conducted at the Boundary Layer Wind-Tunnel Laboratory (BLTWL) in the period 1988-90. Parameters for the TLP used in the experiments are given in Table 1 and the experimental model is shown in Fig. 1 (Ref. 4)

PROPERTY	MODEL
Mass m	6.585 kg
Displacement Δ	9.050 kg
Riser Tension T_{01}	8.42 N
Total Tendon Pretension T_{02}	16.12 N
Water Plane Area A	0.03704 m^2
Deck Size	0.00968 m^2
Centre of Gravity COG	0.263 m
Radius of Gyration x-axis	0.242 m
Radius of Gyration y-axis	0.243 m
Radius of Gyration z-axis	0.235 m
Pontoon Width W_p	0.047 m
Pontoon Depth D_p	0.035 m
Column Centre Line Spacing l_c	0.381 m
Column Height H_c	0.416 m
Column Diameter D_c	0.109 m
Tendon length l_t	3.240 m
Deck depth D_d	0.069 m
Draft D	0.195 m
Water Depth at model d	3.430 m
Water Depth in channel d_c	1.690 m

Table 1: TLP Model Properties

The time history data from the model tests was transmitted to Det Norske Veritas Research AS by means of a magnetic tape, referred to as the "TLPTIM" tape. Spot checks on this data at DNVR show good agreement with the data given in Ref. 6.

The wind sensor 'far pitot' and the wave probe 'wave near' are used in this report to compare measured wind and wave spectra with the simulated wind and wave spectra, used to generate the excitation forces.

No direct test of the surge natural frequency was included in the data from the original tests, but a natural frequency of ~0.1Hz could be inferred from the motion response in wind and irregular waves. In the subsequent damping experiments (Ref. 5) the natural frequency for the TLP was intended to be 0.143Hz. To attain this period the mass was adjusted. From the damping experiments performed without waves the natural frequency can be measured to ~0.156Hz.

Thus, it seems that the surge natural frequency differs between the original model tests in wind and irregular waves, and the subsequent damping tests. Since a comparison with the tests in wind and irregular waves is intended here, the natural frequency of ~0.1Hz from these tests is adopted for use in the present numerical analysis.

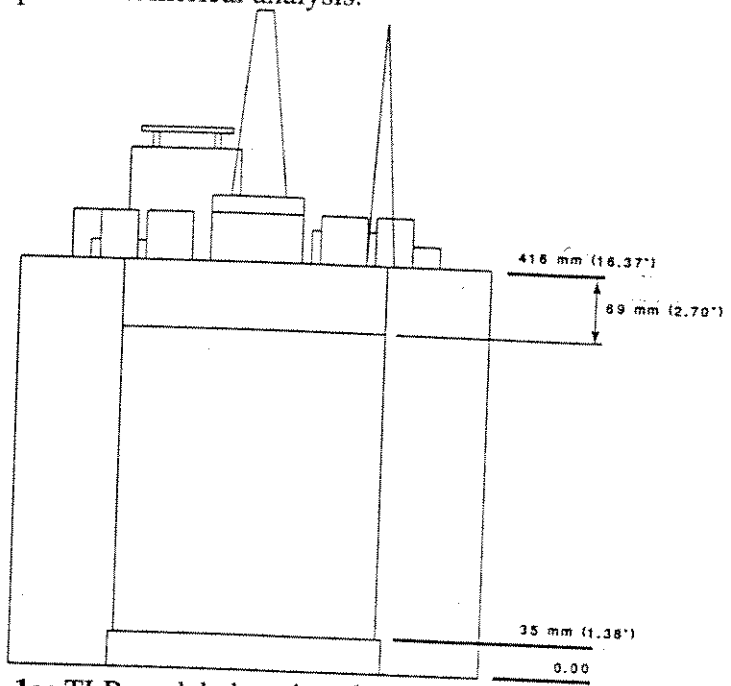

Fig. 1a: TLP model elevation showing principal dimensions

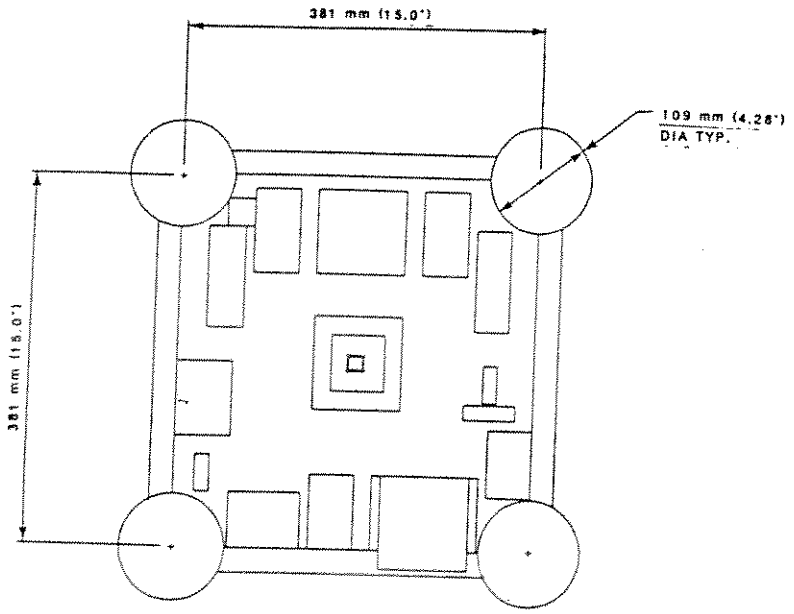

Fig. 1b: TLP model plan showing principal dimensions

4. RESPONSE IN REGULAR WAVES

The response of the TLP in regular waves is calculated by WADAM (Ref. 1). As mentioned earlier this is a diffraction and Morison theory program for the analysis of the interaction of surface waves with offshore structures. The input to WADAM is given in appendix A.

4.1. Panel Model of TLP

Drawings and data describing a generic TLP were provided by BLWT, as reproduced in their report (Ref. 4). A panel model of the TLP was generated from these data, using the Sesam preprocessor PREFEM (Ref. 2). Since the wet part of the TLP has two planes of symmetry, it was only necessary to model one quadrant of the vessel.

Principal dimensions of the TLP are taken from Table 1 and Fig. 1. Component surfaces of the panel model below the water surface are shown in Fig. 2. Each quadrant is composed of 542 panels with all panels wet.

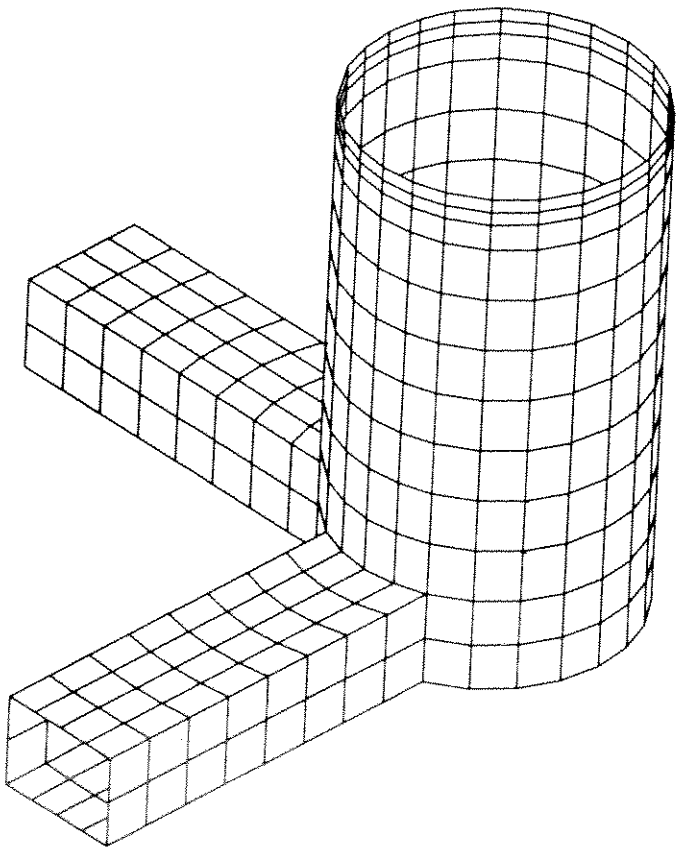

Fig. 2: One quadrant of the model used in the WADAM calculation.

4.2. First Order Transfer Functions

The transfer function for the surge motion calculated by WADAM (ref. 1) is given in Fig. 3. Note that the abscissa is given in radians per second, and the ordinate gives the ratio of surge amplitude to wave amplitude. This transfer function may be compared with the corresponding model test results in Fig.6.1.2 and Fig.6.1.8 of Ref.7. There is reasonable agreement, except at a frequency of about 8 rad/s, where the model tests show much higher response. The model test results at this frequency seem questionable, since the addition of wind leads to a marked reduction in the model test response.

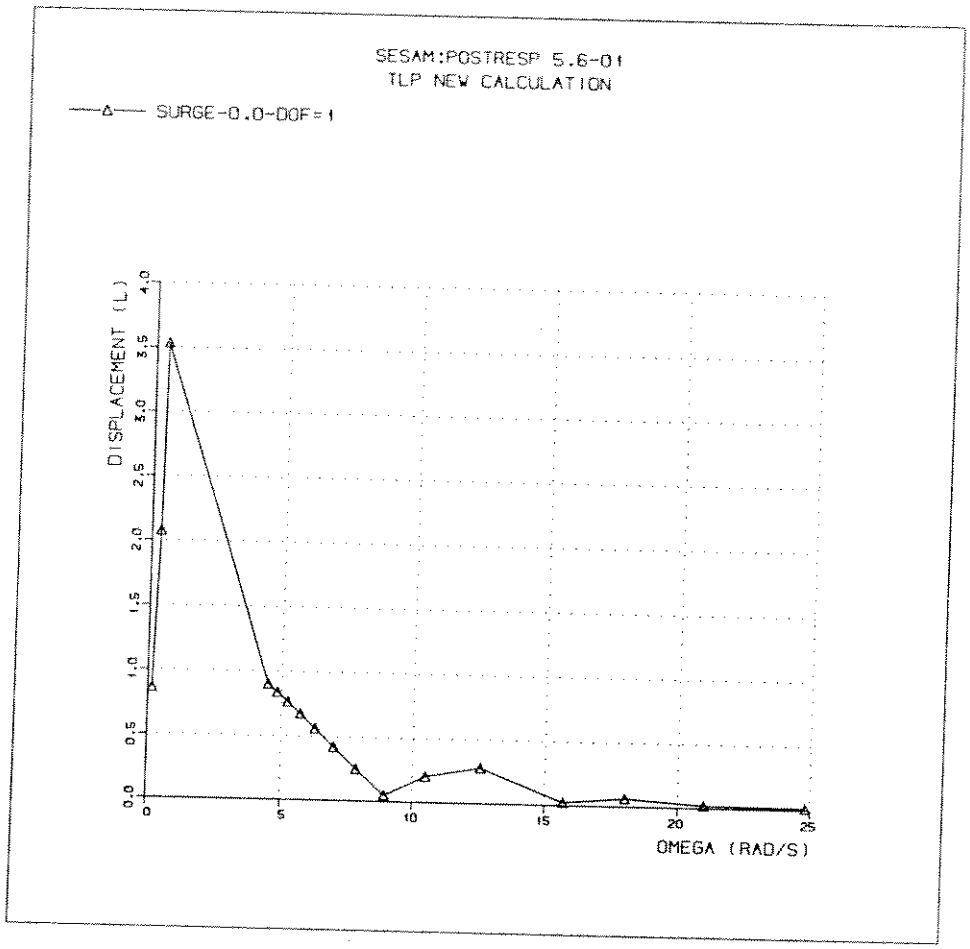

Fig. 3: Transfer function for the surge motion

4.3. Second Order Transfer Functions

The transfer function for the mean drift force calculated by WADAM (ref. 1) is given in Fig. 4. Note that the abscissa is given in radians per second, and the ordinate is gives the ratio of force pr m wave amplitude squared.

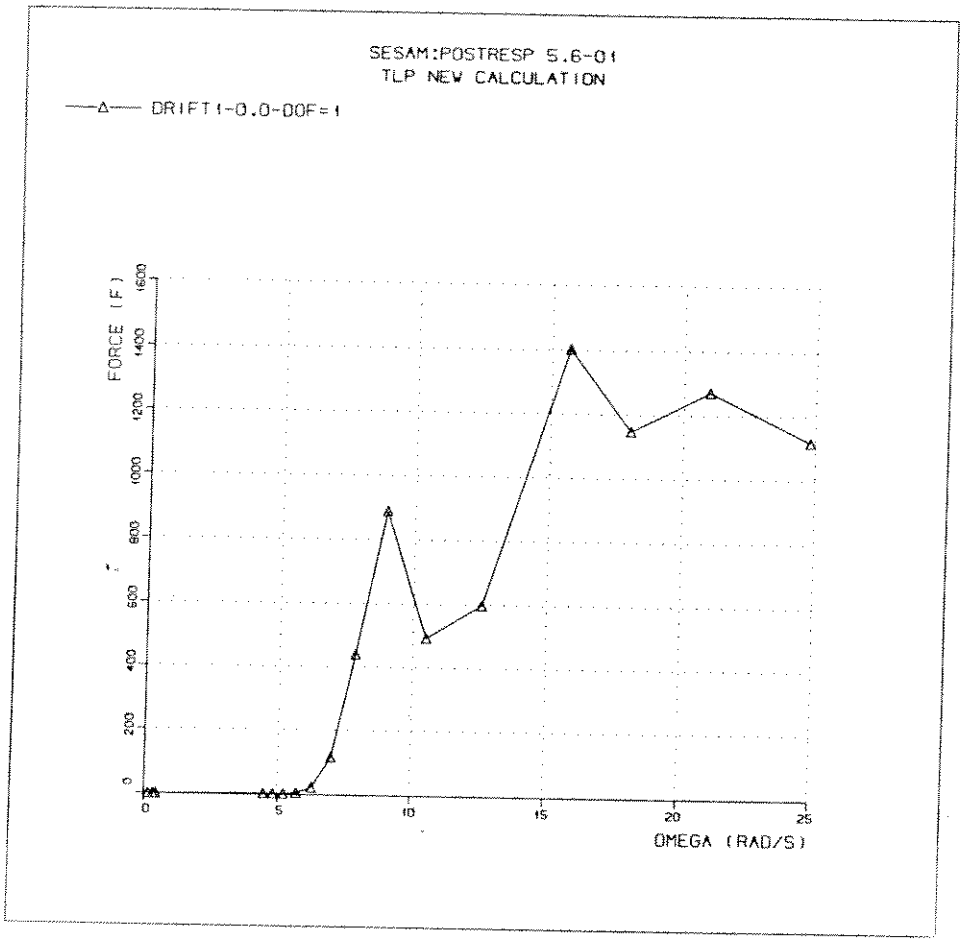

Fig. 4: Transfer function for the mean drift force

5. INPUT PARAMETERS FOR SIMULATION

Most of the input parameters for the simulations are taken from the experiments. Only the surge motion of the TLP is simulated, and therefore the emphasis has been on generating input to the numerical model that is intended to reproduce this degree of freedom as well as possible.

A complete input file for NV1427 is given in Appendix B. Note that the numbers in the input file are non-dimensionalized according to NV1427's standard.

5.1. Radii of Gyration

The radii of gyration for roll and pitch are taken from the experiments as given in Table 1. To avoid numerical problems in the NV1427 program the yaw radius of gyration is increased by a factor 10 compared with the experiments. This will not influence the surge motion.

5.2. Restoring Forces

The mooring stiffness is taken from the experiments. The restoring forces were assumed linear and it was decided to neglect all cross-coupling terms.

Surge and sway restoring force coefficient:

$$R_{11} = R_{22} = \frac{\delta F}{\delta x} = \left(\frac{l_t^3}{(l_t^2 - x^2)^{3/2}} \right) \cdot \left(\frac{(T_{01} + T_{02})}{l_t} + \rho g A \right) - \rho g A = 8.1 \frac{N}{m}$$

The notation and numerical values are taken from Table 1, with an assumed surge/sway displacement: x=0.10 m

The surge and sway restoring force coefficients can also be taken directly from Table 3.1 in Ref. 7: $R_{11}=R_{22}=8.0$ N/m (the inverse of the number in the table).

5.3. Added Mass

WADAM calculates frequency-dependent added mass coefficients for the structure. The added mass coefficients used as input to NV1427 are not frequency-dependent. Since the most critical frequency for the TLP is the natural frequency, the added mass coefficients (value 0.8062 for surge) for this frequency (0.1Hz) are given as input to NV1427. The added mass coefficients are non-dimensionalized wrt. to the structure's mass.

5.4. Hydrodynamic Damping

The hydrodynamic damping coefficients are given as linear coefficients and all cross-coupling terms are neglected. The surge and sway linear damping coefficients depends on the sea state and are taken from Fig. 3.1 in Ref. 6 (The structural damping component due to the rig used in the damping tests has been subtracted):

	Effective linear damping coefficient [N/(m/s)]	Non-dimensionalized after NV1427's criteria
No waves	3.8	0.044
Sea state 1, H_{RMS}=1.4 cm	5.3	0.060
Sea state 2, H_{RMS}=2.0 cm	7.0	0.080

The other damping coefficients will not influence the surge motion and they are given as small coefficients.

5.5. Aerodynamic Drag

Model tests to determine aerodynamic drag coefficients had been carried out in both a "dry" aerodynamic wind tunnel, and in the combined wind and wave facility over water ("wet" tests). The most extensive aerodynamic tests had been carried out in the "dry" wind tunnel and it was originally the intention to use drag coefficients from these tests in the numerical simulations. However, preliminary calculations indicated that the aerodynamic drag force would be significantly underestimated. Comparison of the results from the two types of tests were made, and showed an increase in 23% of the drag coefficient in the "wet" tests, after corrections for the stem attachment in the "dry" tests, and for the different wind speed reference heights. On this basis, it was decided to use drag coefficients from the "wet" tests in the numerical simulations.

The drag coefficients are taken from Table 4.4 in Ref. 9. The wind speed in that report is referred to 0.156 m above water level while the wind probes in the experiments were placed at 0.230 m above mean water level. To adjust for this height difference the drag force coefficients are decreased by 4% based on Fig.3.2.2. in Ref. 4.

The wind load coefficients given in Ref. 9 are given for different wave heights and as mean wind load coefficients and fluctuating wind load coefficients. Since the coefficients do not vary significantly with the wave height, the coefficients for high waves and mean wind coefficients are chosen as input to NV1427. NV1427 does not differentiate between drag coefficients for mean and fluctuating loads. The mean coefficient is chosen here. This should be best for the mean surge response but will tend to overestimate the low frequency surge response to wind.

In Ref. 9 and Ref. 10 Table 3.1.3.1 the drag force coefficients are given for the deck only (no legs). In Ref. 10 Table 3.1.1.1 the drag force coefficients are given for the TLP above the mean water level (both deck and legs). To adjust the drag force coefficients to include the legs the surge aerodynamic drag force coefficient is increased by a factor 1.4.

5.6. Environmental Conditions

Wave spectra and wind speed are taken from Ref. 4 and Ref. 6.

The experimental wave spectra are shown in Ref. 4 for the different sea states and fitted to Jonswap spectra. Peak period (from eq. 4.93 in Ref. 13) and significant wave height are calculated from these formulas:

$$T_p = (1.49 - 0.102\gamma + 0.0142\gamma^2 - 0.00079\gamma^3) \cdot T_z$$

$$H_s = 4 \cdot H_{rms}$$

Wave periods and γ–values are taken from Ref. 4 while wave heights are taken from Ref. 6.

The experimental and simulated wave spectra are shown in Fig.19, 25, 28, and 31. The figures show reasonable agreement between experimental and numerical wave spectra, with somewhat more energy concentrated at the peak of the experimental data.

The wind spectra are simulated using Harris wind spectra and the input parameters to NV1427 are tuned to fit the experimental wind spectra. The wind speeds are taken from Ref. 6. The simulation of the wind spectrum is based on the wind spectrum measured at "far pitot". Since the natural surge frequency for the TLP is 0.1Hz the spectra measured at "far pitot" can be used without correction of the wind spectra (Ref. 11).

The experimental and simulated wind spectra are shown in Fig.11, 17, 27, 30. In general, the figures show that the experimental and simulated wind spectra agree reasonably well. The excitation around the natural surge frequency of 0.1Hz is most critical. At this frequency the simulated wind spectra tend to provide slightly less energy than the experimental wind spectra do in the presence of waves (Fig.27 and 30).

The deviations between the simulated and experimental wind and wave spectra have to be taken into account when one compares the experimental surge motions with the calculated motions.

6. RESULTS OF TIME-DOMAIN MOTION SIMULATIONS

The main response statistics from the simulations are given in Tables 2-4 and in Figs. 5-10. Table 2 and Fig.5-6 refer to wind only, Table 3 and Fig.7-8 refer to waves only, and Table 4 and Fig.9-10 refer to waves and wind. A frequency of 0.4Hz has been chosen as the boundary separating low frequency and wave frequency effects. In both tables and figures, low frequency implies the standard deviation obtained by integrating the response spectra upto the boundary frequency of 0.4Hz. Wave frequency implies the standard deviation from above 0.4Hz.

In Fig.11-28 the simulated and experimental wind spectra, wave spectra, and surge response spectra are given for the different sea states and wind speeds. These figures are placed at the end of the report, while Fig.5-10, are interspersed with the text.

6.1. Wind Only

In the experiments for the case "wind only" the wind generates small wind-induced waves. In the simulations no waves are given as input. As can be seen from Table 2 the wind-induced waves are small and will not influence the surge motion significantly.

WIND ONLY		wind speed u=1.7 m/s		wind speed u=3.9 m/s	
		experimental	numerical	experimental	numerical
WIND [m/s]	mean speed	1.698	1.690	3.889	3.900
	st. deviation	0.191	0.188	0.401	0.425
	Low freq.	0.175	0.166	0.340	0.323
WAVE [m]	mean elevation	-0.002	0.000	-0.002	0.000
	st. deviation	0.002	0.000	0.006	0.000
	Low freq.	0.002	0.000	0.001	0.000
	Wave freq.	0.001	0.000	0.006	0.000
SURGE MOTION [m]	mean drift	0.026	0.024	0.133	0.127
	st. deviation	0.008	0.006	0.019	0.026
	Low freq.	0.008	0.006	0.019	0.027
	Wave freq.	0.000	0.000	0.000	0.000

Table 2: Comparison of experiments with simulations of excitation and surge motion of the TLP in wind only.

Samples of the time histories are shown in Fig.13-16. The wind speeds in Fig.13 and Fig.14 seem fairly similar. The experimental surge signal in Fig.15 contains some high frequency noise which is absent from the simulated surge in Fig.16. This noise seems to occur at frequencies exceeding the cut-off frequency of 1.6Hz, used for the response spectra in Fig.12. It may possibly be excited by wind-induced waves with a relatively high frequency. Otherwise, the mean and low-frequency surge response appear comparable.

Fig.5 shows good agreement in the mean surge displacement. This indicates satisfactory modeling of the mean wind force, and of the restoring force due to the tethers.

Surge motion statistics in Table 2 confirm that the wind excitation only generates significant response in the low frequency band, both in the experiments and in the simulations.

As can be seen from Fig.6, 12, and 18 the simulated response spectra are smaller than the experimental results for low mean wind speeds and larger for higher wind speeds. No aerodynamic damping force is used in the simulations. The aerodynamic damping force is more significant at larger wind speeds. This can partly explain why simulated response spectra are smaller for small wind speeds and larger for higher wind speeds. The differences in experimental and simulated wind spectra in Fig.11 and Fig.17 are also partly responsible for the differences in response. The use of the mean-based drag force coefficient to generate both mean and fluctuating wind forces is also expected to lead to some overestimation of the fluctuating wind forces.

The response spectra in Fig.12 and Fig.18 also indicate reasonable agreement in the resonance frequency, between experiments and simulations, at about 0.1Hz. This tends to confirm that the numerical modeling of the dry inertia, added-mass, and restoring forces agrees reasonably well with the experimental model.

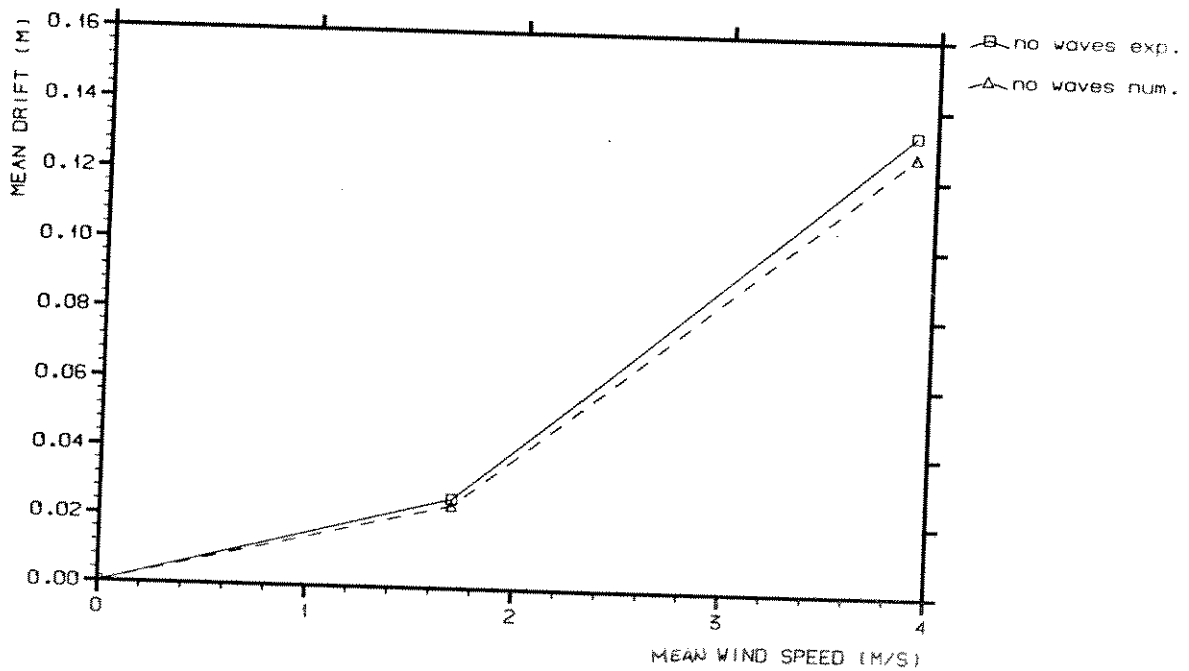

Fig. 5: Comparison of experimental and simulated mean surge displacement. Wind only.

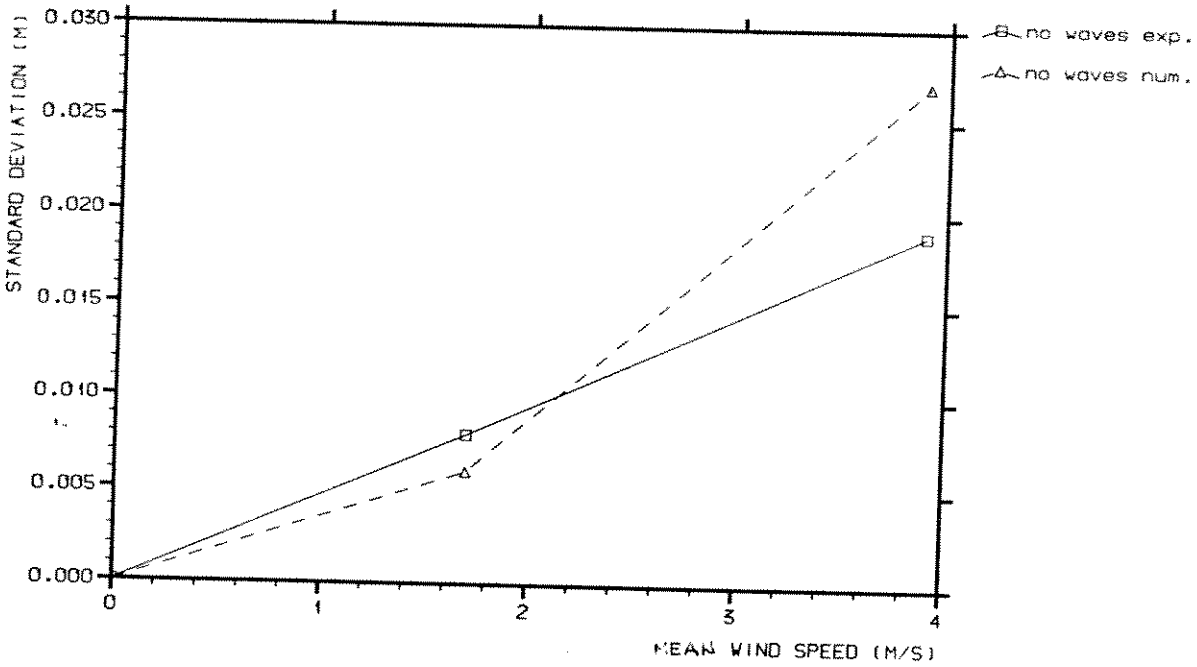

Fig. 6: Comparison of experimental and simulated surge motion for low frequencies. Wind only, standard deviation.

6.2. Waves Only

The experiments given in Table 3 were supposed to be without any wind speed. However, the wind probe "far pitot" measured non-zero wind speeds. How this wind is generated and measured is unknown to the author and it is therefore difficult to estimate how this wind speed influences the surge motion of the TLP. A rough estimate of the effect of this wind can tentatively be based on the ratios of the wind velocities; viz. 0.275:1.698=1:6 for comparison of the first columns of Tables 3 and 2. The mean wind-induced surge is proportional to the velocity squared; i.e. about 0.026/36=0.001 m, or about 4% of the mean wave-induced surge. The low-frequency surge might be assumed proportional to the wind velocity, itself; i.e. about 0.008/6=0.001m or about 6% of the low-frequency wave-induced surge. Although these estimates are very rough, they tend to indicate that the effects of the extra wind loads are fairly small.

Sample time histories are shown in Fig.21-24. The characteristics of experimental and simulated signals for both wave elevation and surge motion appear similar in these figures.

The two wave spectra considered in these tests have different wave periods. The mean wave-induced drift force tends to decrease with increase in wave period, while it increases with increase wave height. This is the basis for the variation of the simulated mean surge in Fig.7. However, the experimental mean surge does not show quite the same trend. There is also a somewhat similar difference in the standard deviation of the low-frequency surge motion in Fig.8. In this case, the modeling of the damping in the numerical simulations also affects the trend with wave conditions. A larger damping coefficient is applied in the higher waves, as described in section 5.4. It may well be that the increase in damping coefficients, inferred from the damping tests (Ref.5) is exces-

sive. Some other potential sources of differences are: (a) viscous excitation forces in the model tests, (b) effects due to finite wave elevation, and (c) coupled modes of motion due to non-uniform tether stiffness.

WAVES ONLY		H_s=0.061 m, T_p=0.99 s		H_s=0.086 m, T_p=1.19 s	
		experimental	numerical	experimental	numerical
WIND [m/s]	mean speed	0.275	0.000	0.197	0.000
	st. deviation	0.209	0.000	0.211	0.000
	Low freq.	0.221	0.000	0.209	0.000
SEA STATE [m]	mean elevation	0.000	0.000	0.000	0.000
	st. deviation	0.015	0.017	0.021	0.021
	Low freq.	0.001	0.001	0.001	0.001
	Wave freq.	0.015	0.017	0.021	0.021
SURGE MOTION [m]	mean drift	0.016	0.023	0.016	0.009
	st. deviation	0.022	0.020	0.026	0.018
	Low freq.	0.021	0.018	0.021	0.009
	Wave freq.	0.007	0.009	0.015	0.015

Table 3: Comparison of the experiments with simulations of excitation and surge motions of the TLP in waves only.

The difference between the experimental and simulated low-frequency surge motion is also clearly shown in the response spectra in Fig.20 and Fig.26. These two figures also illustrate the very good agreement in the surge motion in the wave-frequency band.

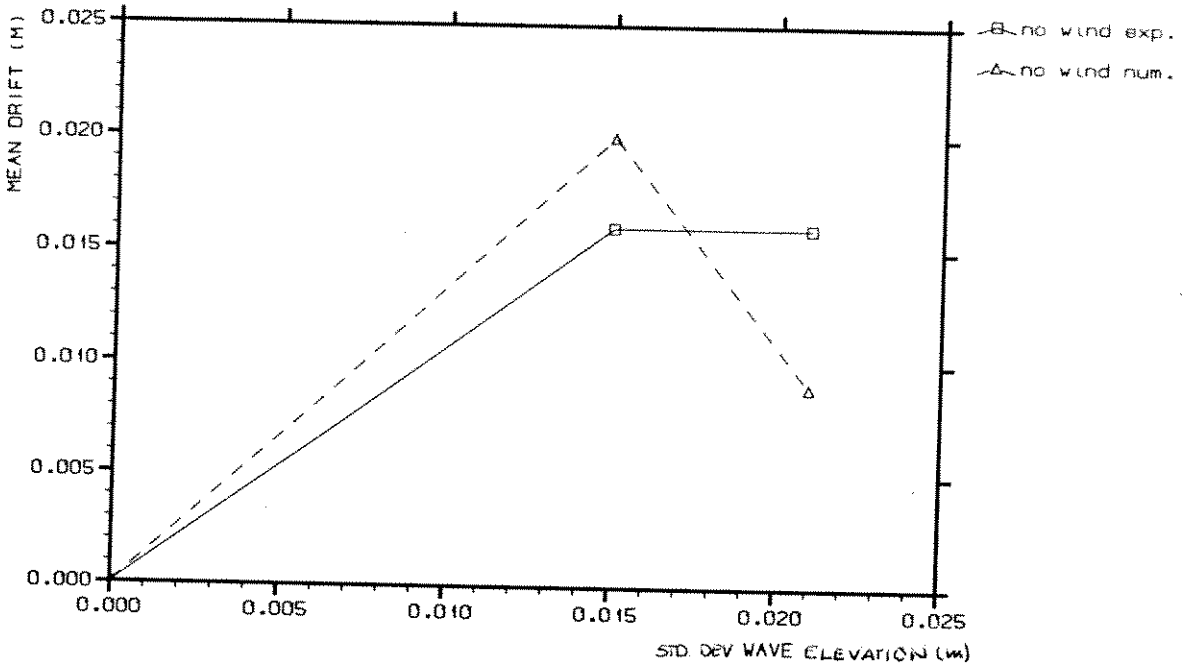

Fig. 7: Comparison of experimental and simulated surge motion for low frequencies. Waves only, mean drift.

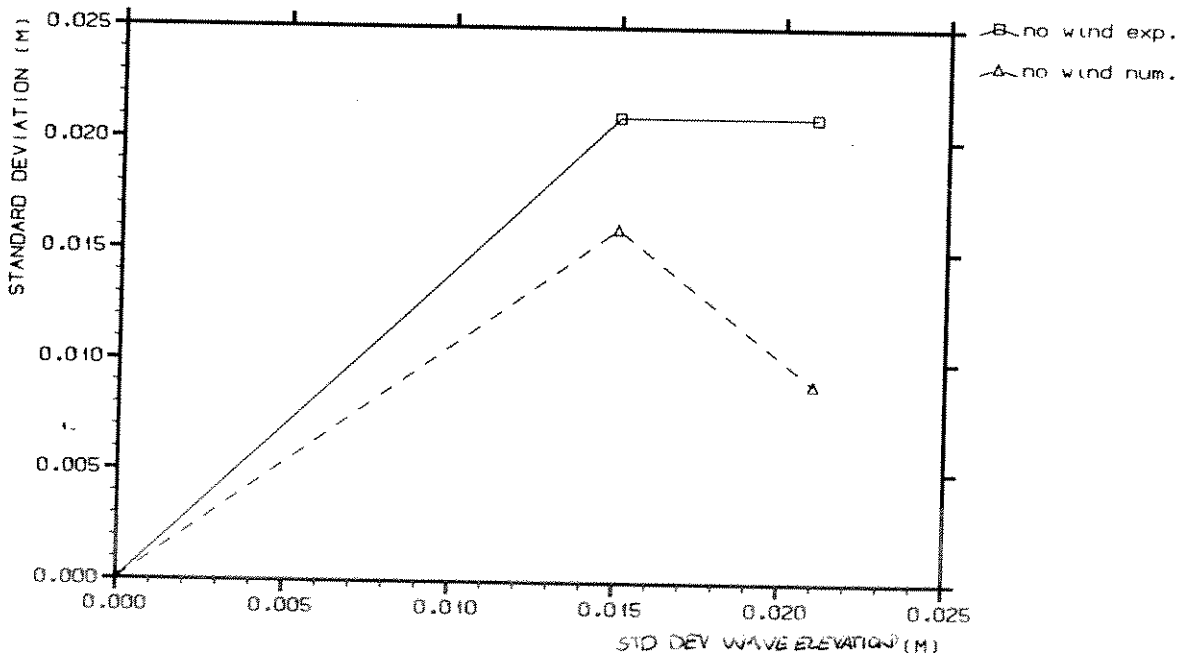

Fig. 8: Comparison of experimental and simulated surge motion for low frequencies. Waves only, standard deviation.

6.3. Wind and Waves

Sample time traces of wind, waves, and surge response from experiments and simulations are shown in Fig.33-38. The characteristics of the signals appear fairly similar, though there is a slight indication of some high frequency content in the experiments which seems absent from the simulations.

Fig.9 shows good agreement in the mean surge displacement between experiments and model tests. The mean surge displacement is dominated by the wind-induced mean force, so that the discrepancy seen in the wave-induced mean surge, in Fig.7, is no longer significant.

WIND AND WAVES		H_s=0.057 m, T_p=0.99 s wind speed u=3.9 m/s		H_s=0.087 m, T_p=1.19 s wind speed u=3.9 m/s	
		experimental	numerical	experimental	numerical
WIND [m/s]	mean speed	3.938	3.930	3.885	3.880
	st. deviation	0.402	0.428	0.406	0.423
	Low freq.	0.349	0.325	0.340	0.322
WAVE [m]	mean elevation	0.000	0.000	0.000	0.000
	st. deviation	0.014	0.014	0.022	0.022
	Low freq.	0.001	0.001	0.002	0.001
	Wave freq.	0.014	0.014	0.022	0.022
SURGE MOTION [m]	mean drift	0.129	0.145	0.137	0.136
	st. deviation	0.023	0.027	0.027	0.026
	Low freq.	0.022	0.026	0.024	0.022
	Wave freq.	0.006	0.006	0.014	0.014

Table 4: Comparison of the experiments with simulations of excitation and surge motions of the TLP in wind and waves.

The response spectra in Fig.29 and Fig.32 show good agreement for the wave-frequency surge motion, but the low-frequency surge motion differs. The simulations overestimate the response in sea state 1 (H_s=0.057 m, T_p=0.992 s), while they underestimate the response in sea state 2 (H_s=0.087 m, T_p=1.19 s). This behaviour is summarised in Fig.10. The damping model used in the simulations seems to be the best point of attack to improve the numerical predictions.

The relatively slight increase in the low-frequency surge response in combined wind and waves, compared to either excitation mechanism alone, is one of the most interesting aspects of the model test results. The explanation for this behaviour may well lie in interaction due to the damping mechanisms; viz. aerodynamic damping (with a damping coefficient proportional to the wind speed) also tends to damp the wave-induced, low-frequency surge response, and wave drift damping (dependent on wave height) also tends to damp the wind-induced, low-frequency surge.

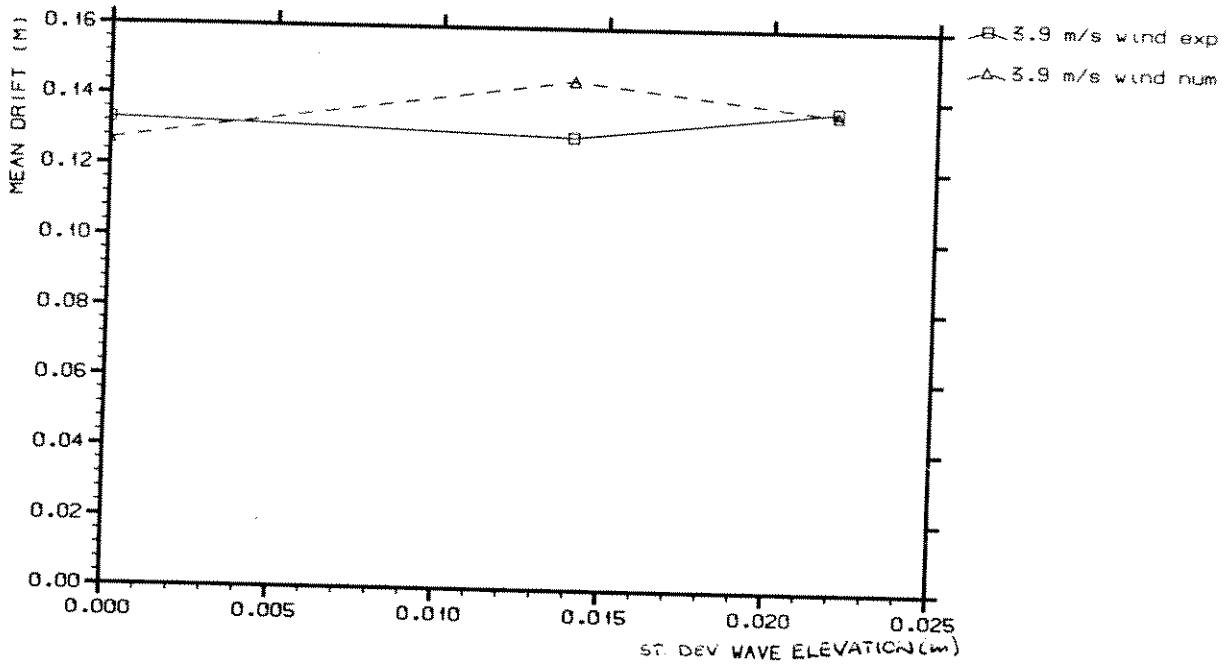

Fig. 9: Comparison of experimental and simulated surge motion for low frequencies. Both wind and waves, standard deviation.

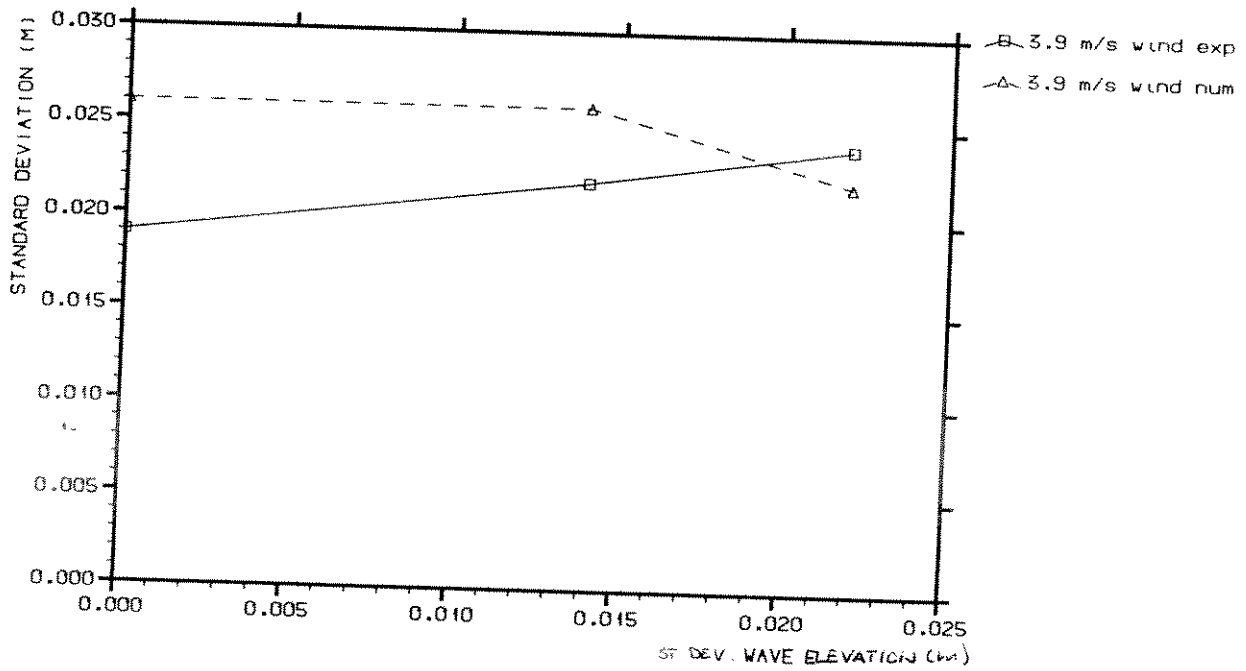

Fig. 10: Comparison of experimental and simulated surge motion for low frequencies. Both wind and waves, standard deviation.

7. CONCLUSIONS

Numerical simulations have been made of the surge motion time histories of a tension leg platform, under the influence of wind and wave loads. The simulation results have been compared with the results of model tests from the Boundary Layer Wind Tunnel Laboratory. The following conclusions may be drawn from the comparison:

1) Satisfactory agreement in surge natural frequency, implying agreement in inertia and restoring properties of both experimental and numerical models.

2) Satisfactory agreement in mean surge due to wind alone, implying agreement in the mean wind loads.

3) Upto 42% difference in the standard deviation of the low-frequency surge motion due to wind alone - that may be partly attributed to the numerical models for both the fluctuating wind force, and for the damping.

4) Upto 77% difference in the mean surge due to waves alone, however, the magnitude is much lower than the wind-induced mean surge, so experimental inaccuracies may be more significant.

5) Upto 43% difference in the standard deviation of the low-frequency surge motion due to waves alone - that may partly be attributed to the numerical model for the damping.

6) Satisfactory agreement in the first order, wave-induced motions, excited in the frequency band of the incoming waves.

7) Satisfactory agreement in the mean surge due to combined wind and waves (which is dominated by the wind load).

8) Fair agreement in the standard deviation of the low-frequency surge motion due to combined wind and waves (which appears fortuitous in view of items 3 and 5 above).

9) Satisfactory agreement in the wave-frequency surge motion, in the presence of combined wind and wave excitation.

Note that the numerical simulations were only dependent on aerodynamic drag coefficients and hydrodynamic damping coefficients from the model tests, and all other aspects of the platform loads and response were numerically calculated.

Recommendations

Numerical models for the simulation of the motion response of offshore platforms to combined wind and wave excitation should: (a) Apply separate drag coefficients for the modeling of mean and fluctuating wind forces, and (b) apply improved damping models, including aerodynamic damping and wave-drift damping, as compared to the program (NV1427) utilized in the present study.

Model testing in a combined wind and wave facility is invaluable to handle the interaction of the damping mechanisms on the motion response. However, more attention to the quantification of the experimental accuracy, and to the evaluation of model scale effects is required. Supplementary tests, at a larger scale, in a waves-only facility might be necessary to quantify the hydrodynamic forces to an acceptable accuracy.

8. REFERENCES

Reference 1: "WADAM - Wave Loading by Diffraction and Morison Theory, User's Manual," Veritec Report No. 86-3420, Høvik, 1986, T.Christiansen.

Reference 2: "PREFEM - Preprocessor for General Finite Element Program, User's Manual," Veritec Report No. 87-3166, Høvik, 1987.

Reference 3: "NV1427 - Dynamic Analysis of Mooring Systems, User's Manual," Veritec Report No. 84-3638, Høvik, 1984, T. Marthinsen.

Reference 4: "Wind/Wave Interaction on Compliant Offshore Structures, Preliminary Report No. 1 -Flow Structure, Sea States Models" BLWT-SS31-1988, Ramsay, S.R., Vickery, B.J., Judge, M.M.

Reference 5: "Hydrodynamic Damping and Wave-Induced Forces" BLWT-SS6-1992, Vickery, B.J., Ng, M., Ramsay, S.R.

Reference 6: "Wind/Wave Interactions on Compliant Offshore Structures, Tension Leg Platform," Boundary Layer Wind Tunnel Laboratory, 1990, London, Ontario.

Reference 7: "Wind/Wave Interaction on Compliant Offshore Structures, Preliminary Report No. 7 -Tension Leg Platform Wind/Wave Tests" BLWT-SS39-1989, Ramsay, S.R., Vickery, B.J., Stark, R.

Reference 8: Telefax from BLWT to Jan Mathisen, VR, date 90.09.10

Reference 9: "Evaluation of Wind Load Models for Compliant Platforms" VR Report No 90-2025, Høvik 1990, Mathisen, J.

Reference 10: "Wind/Wave Interaction on Compliant Offshore Structures, Preliminary Report No. 2 -Aerodynamic Tests - Force Coefficients" BLWT-SS02-1989, Ramsay, S.R., Vickery, B.J., Ng, M.

Reference 11: Telefax from BLWT to Jan Mathisen, VR, date 90.09.25

Reference 12: "Calculation of Slowly Varying Drift Forces" Applied Ocean Research, Vol.5, No.3, 1983, T. Marthinsen.

Reference 13: "Hydrodynamics of Offshore Structures" Computational Mechanisms Publications 1987, Chakrabarti, S.K.

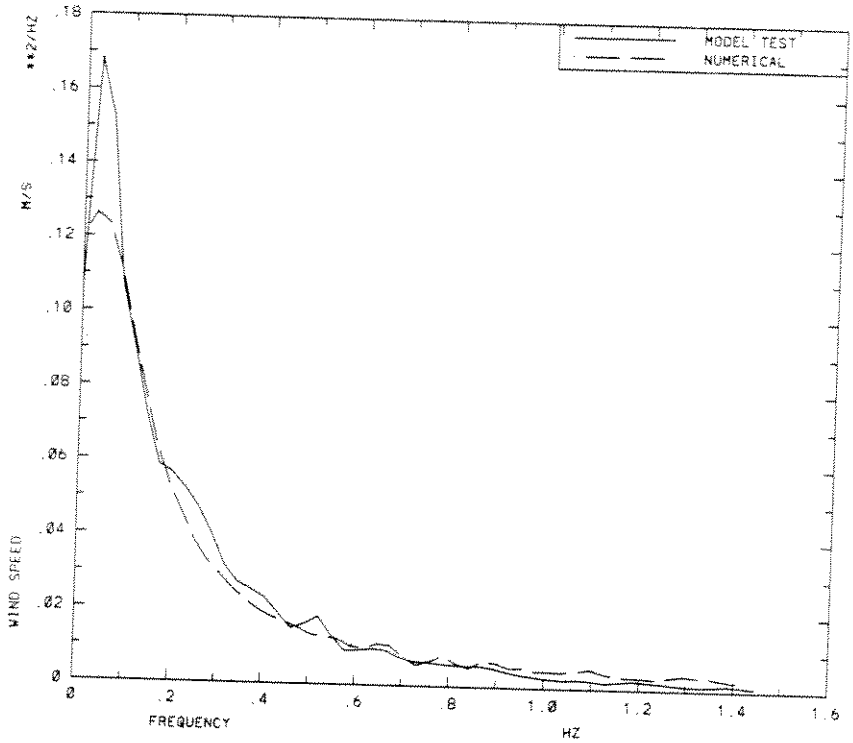

Fig. 11: Comparison of experimental and simulated wind spectra.
Wind speed u=1.7 m/s, no waves.

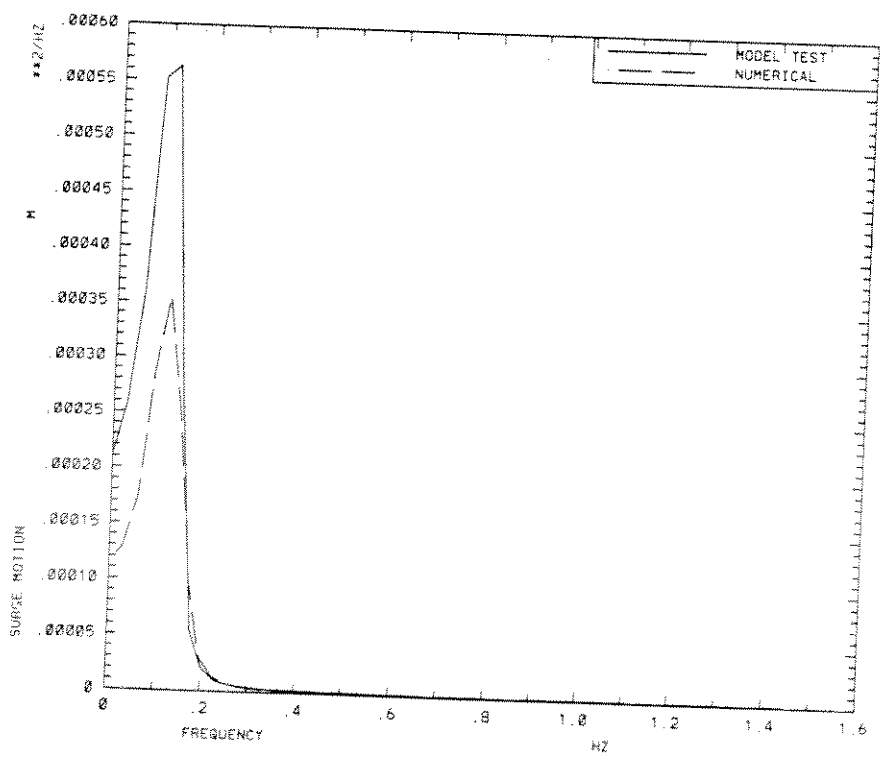

Fig. 12: Comparison of experimental and simulated surge motion spectra.
Wind u=1.7 m/s, no waves.

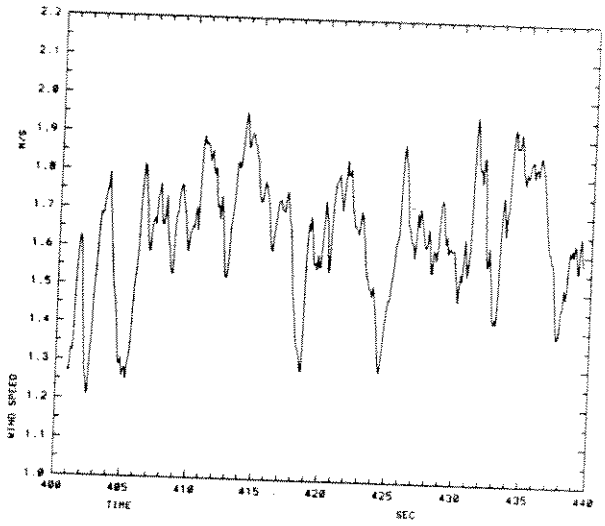

Fig. 13: Time period of experimental wind speed u=1.7 m/s.

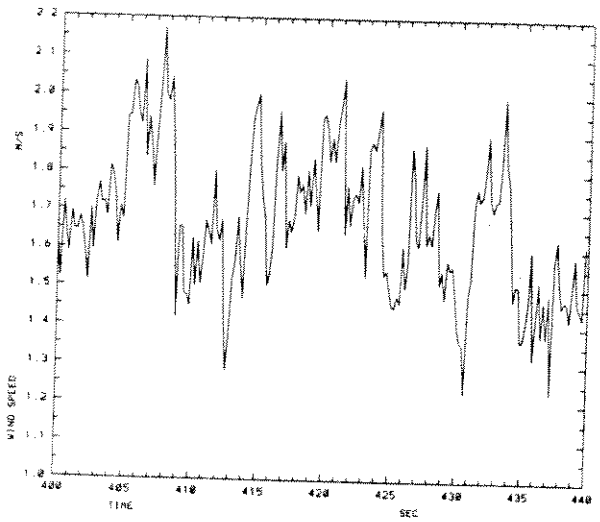

Fig. 14: Time period of simulated wind speed u=1.7m/s.

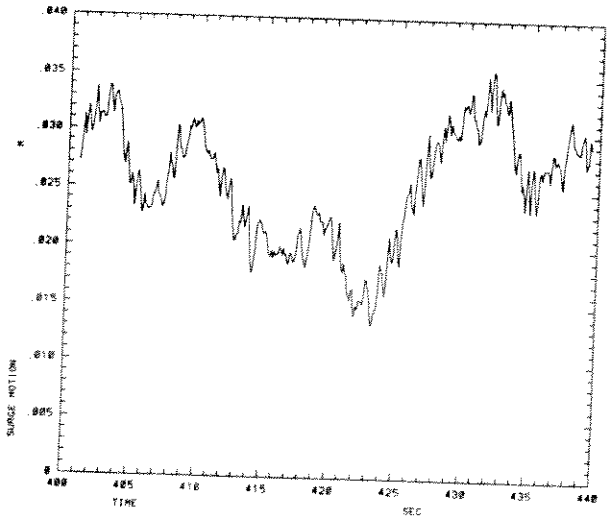

Fig. 15: Time period of experimental surge motion for u=1.7 m/s.

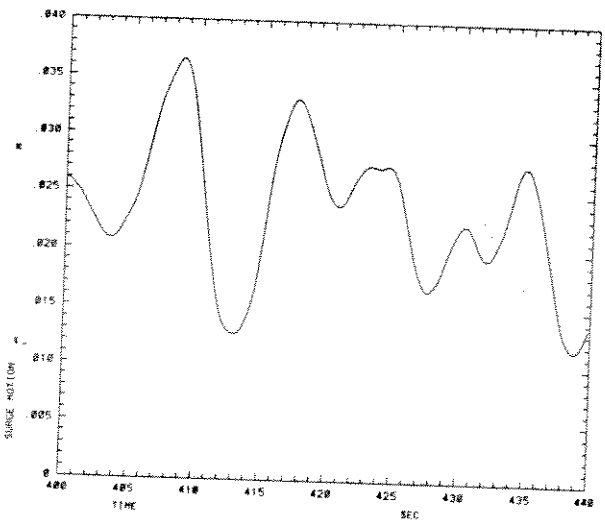

Fig. 16: Time period of simulated surge motion for u=1.7 m/s.

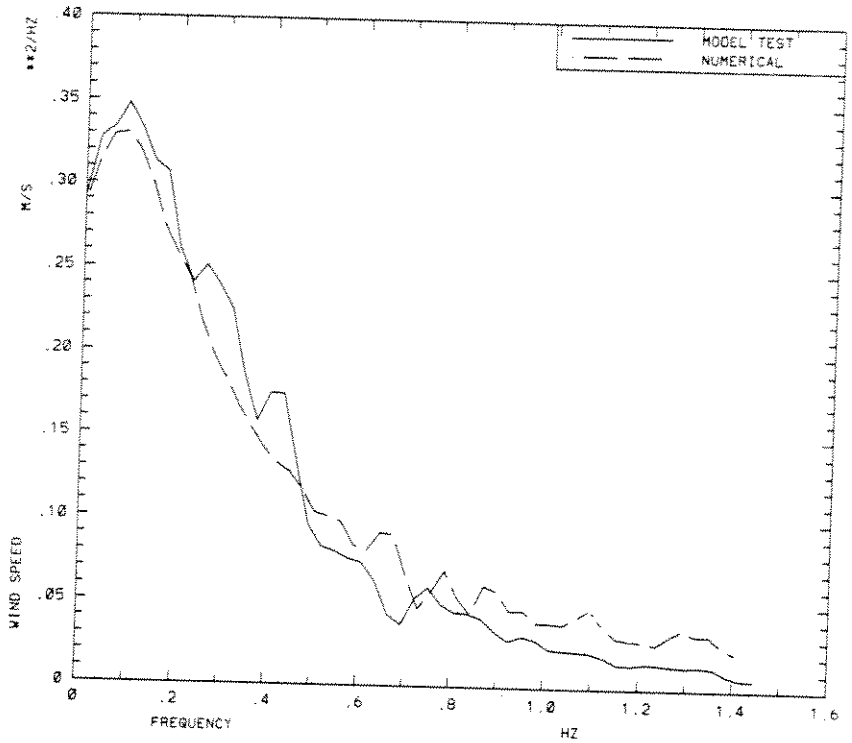

Fig. 17: Comparison of experimental and simulated wind spectra. Wind speed u=3.9 m/s, no waves.

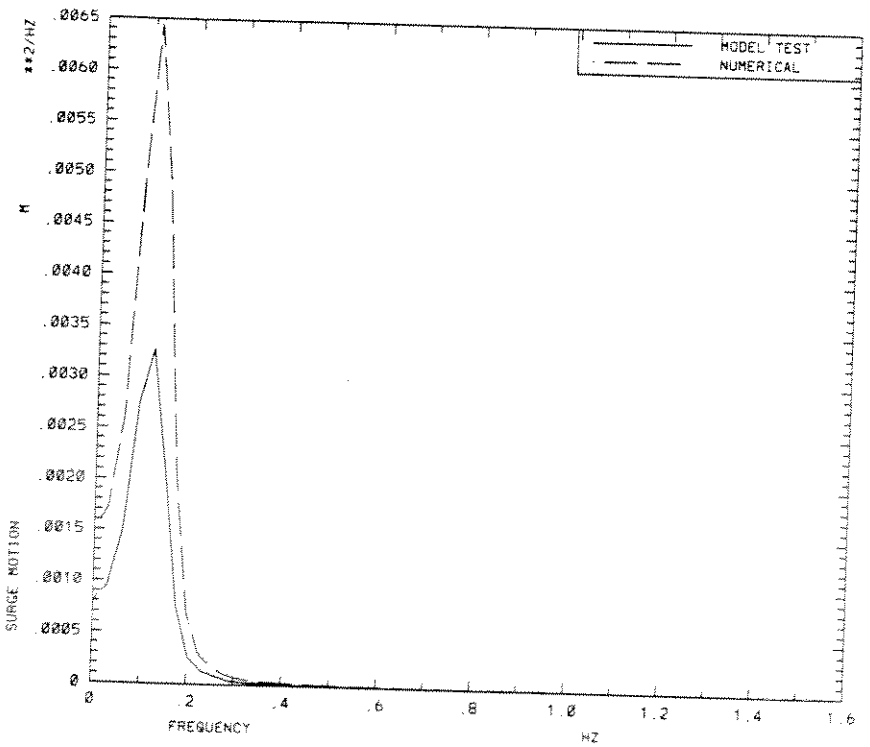

Fig. 18: Comparison of experimental and simulated surge motion spectra. Wind speed u=3.9 m/s, no waves.

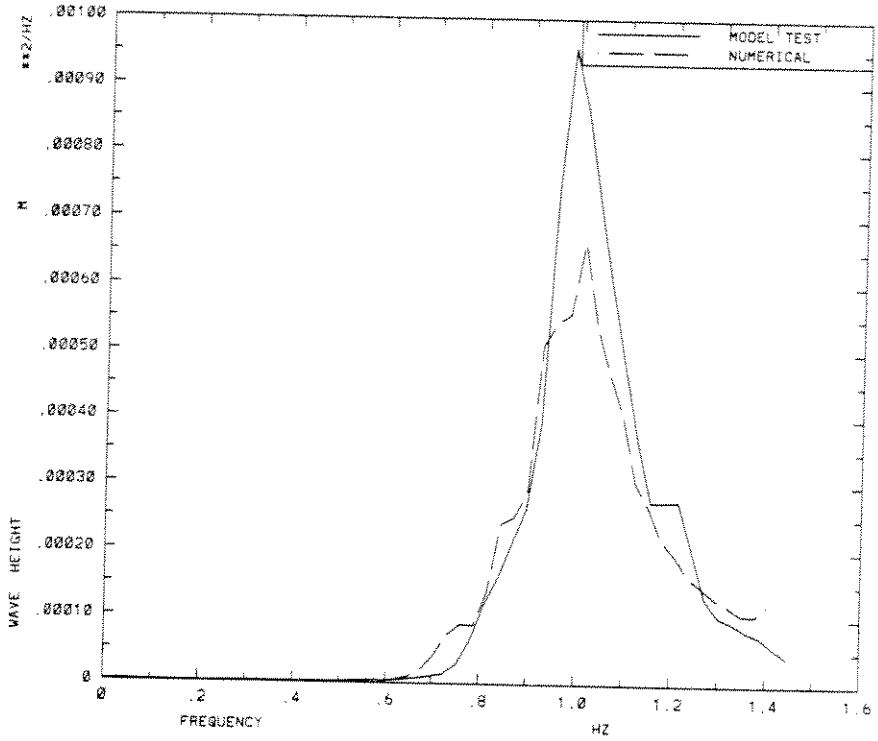

Fig. 19: Comparison of experimental and simulated wave spectra.
No wind, sea state 1, H_s=0.061 m, T_p=0.99 s.

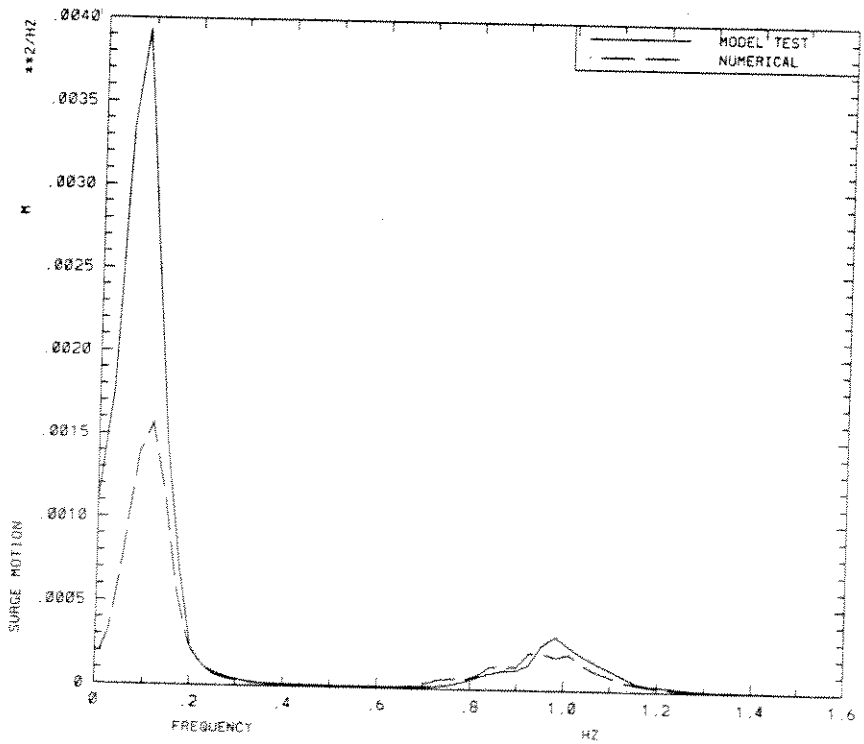

Fig. 20: Comparison of experimental and simulated surge motion spectra.
No wind, sea state 1, H_s=0.061 m, T_p=0.99 s.

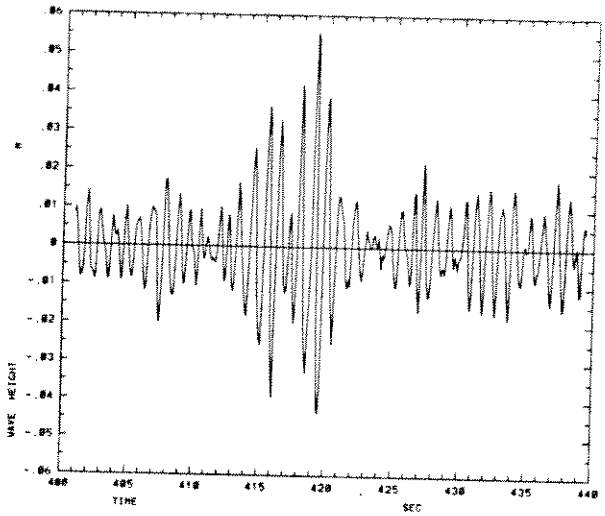

Fig. 21: Time period of experimental wave elevation sea state 1.

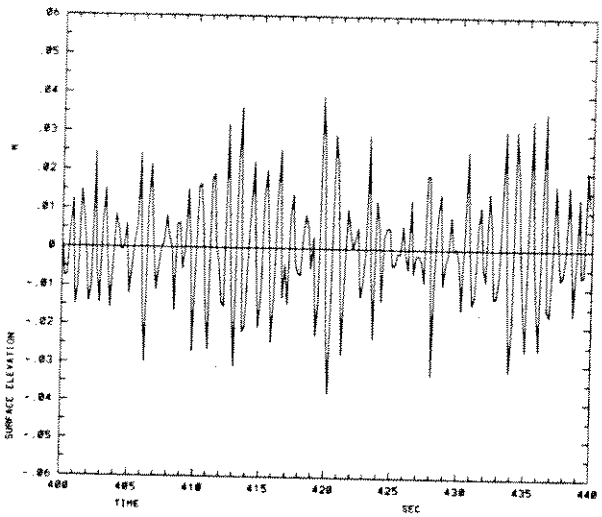

Fig. 22: Time period of simulated wave elevation, sea state 1.

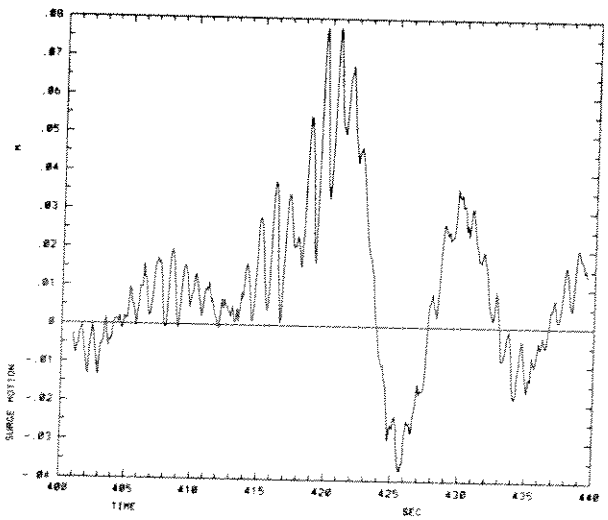

Fig. 23: Time period of experimental surge motion for sea state 1.

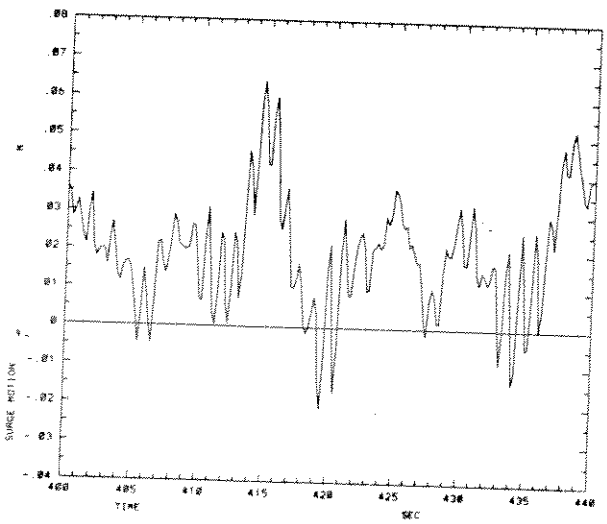

Fig. 24: Time period of simulated surge motion for sea state 1.

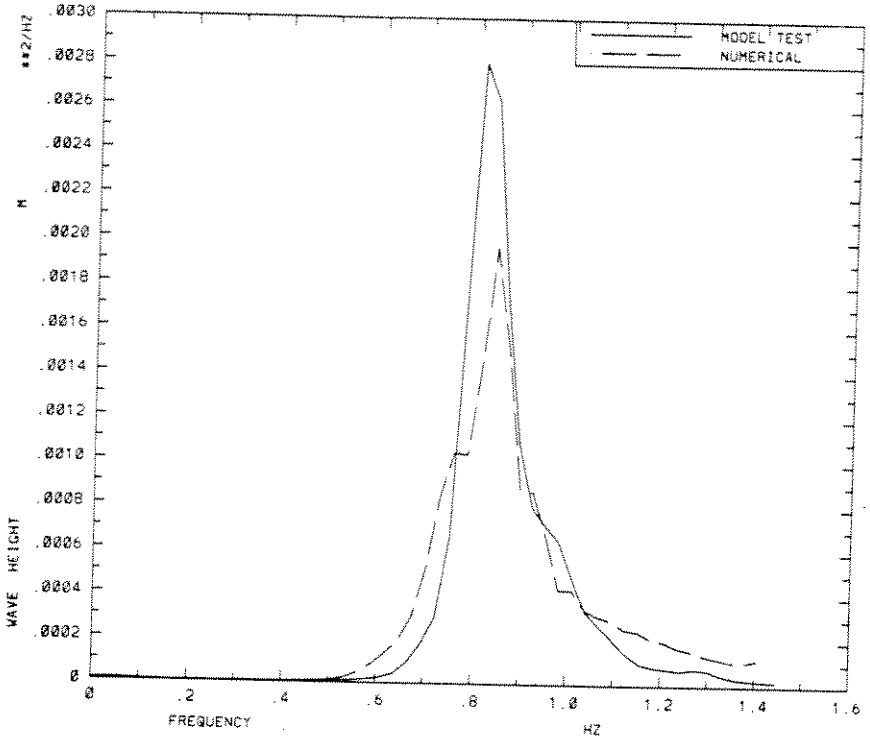

Fig. 25: Comparison of experimental and simulated wave spectra.
No wind, sea state 2, H_s=0.086 m, T_p=1.19 s.

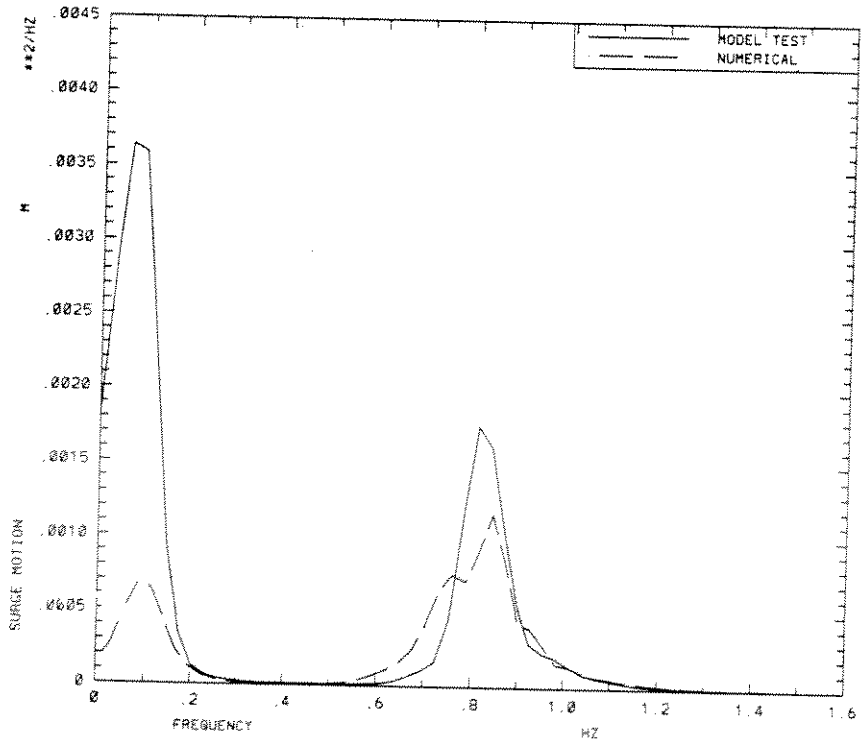

Fig. 26: Comparison of experimental and simulated surge motion spectra.
No wind, sea state 2, H_s=0.086 m, T_p=1.19 s.

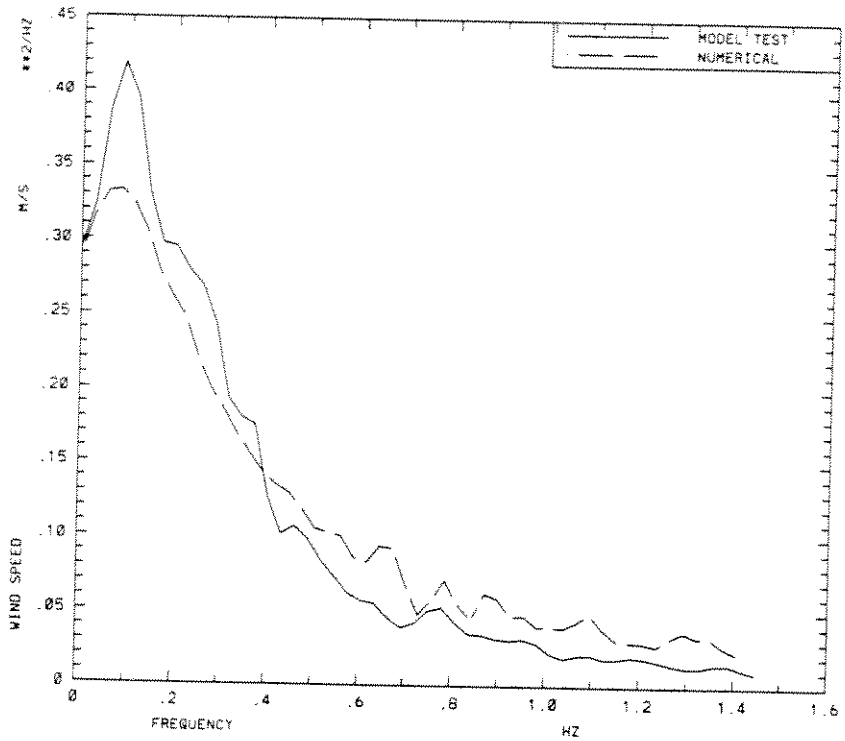

Fig. 27: Comparison of experimental and simulated wind spectra.
Wind speed u=3.9 m/s, sea state 1, H_s=0.057 m, T_p=0.99 s.

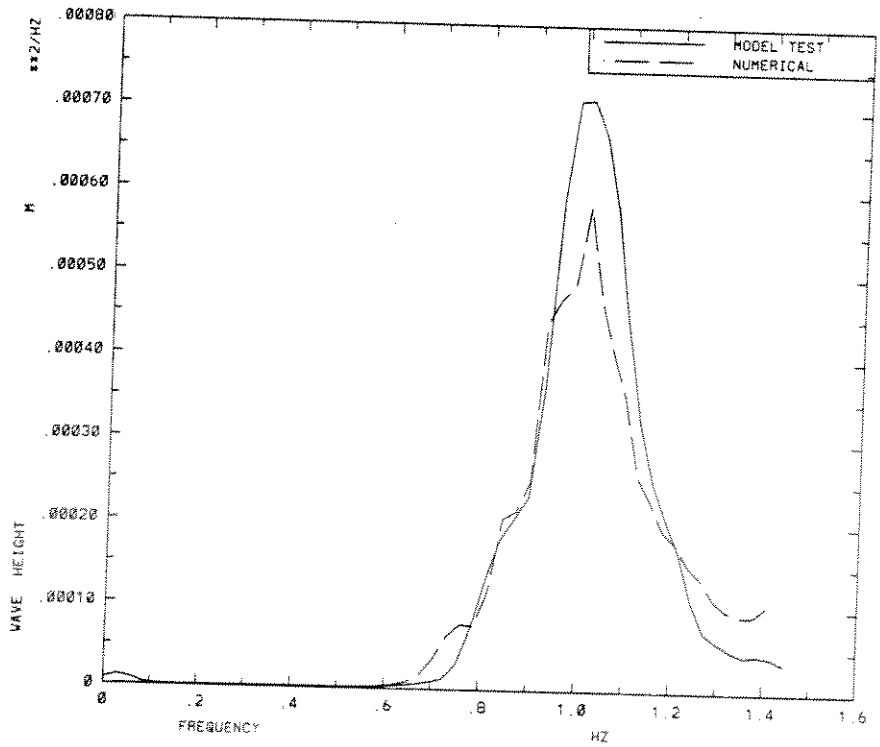

Fig. 28: Comparison of experimental and simulated wave spectra.
Wind speed u=3.9 m/s, sea state 1, H_s=0.057 m, T_p=0.99 s.

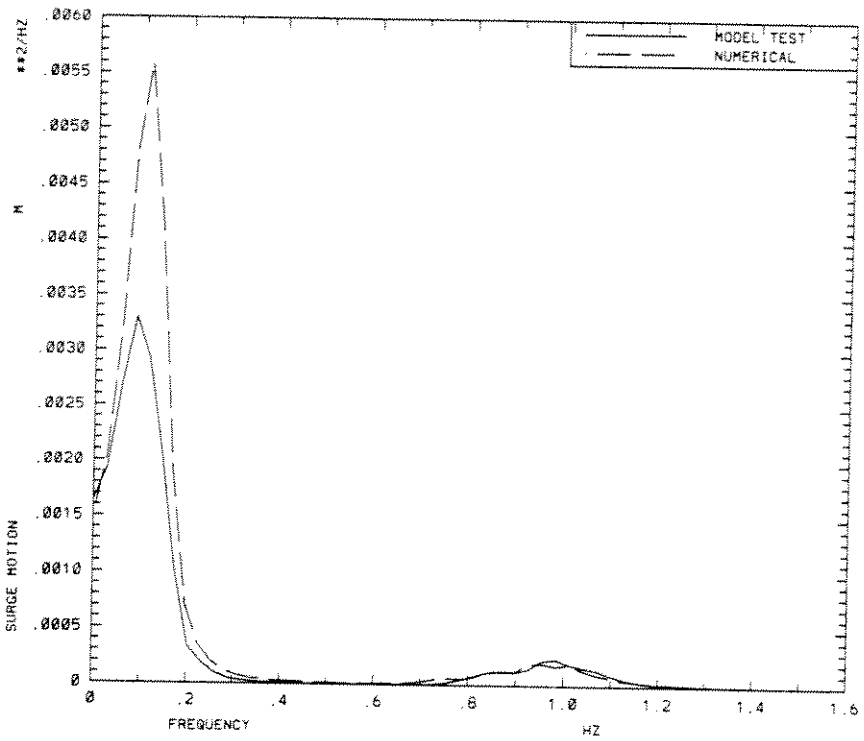

Fig. 29: Comparison of experimental and simulated surge motion spectra. Wind speed u=3.9 m/s, sea state 1, H_s=0.057 m, T_p=0.99 s.

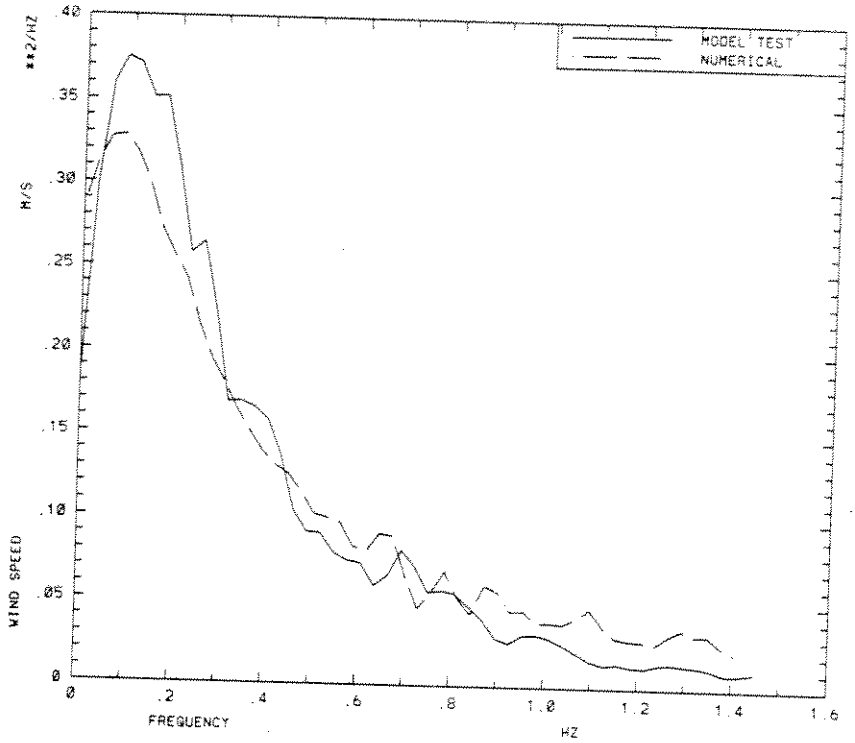

Fig. 30: Comparison of experimental and simulated wind spectra.
Wind speed u=3.9 m/s and sea state 2, H_s=0.087 m, T_p=1.19 s.

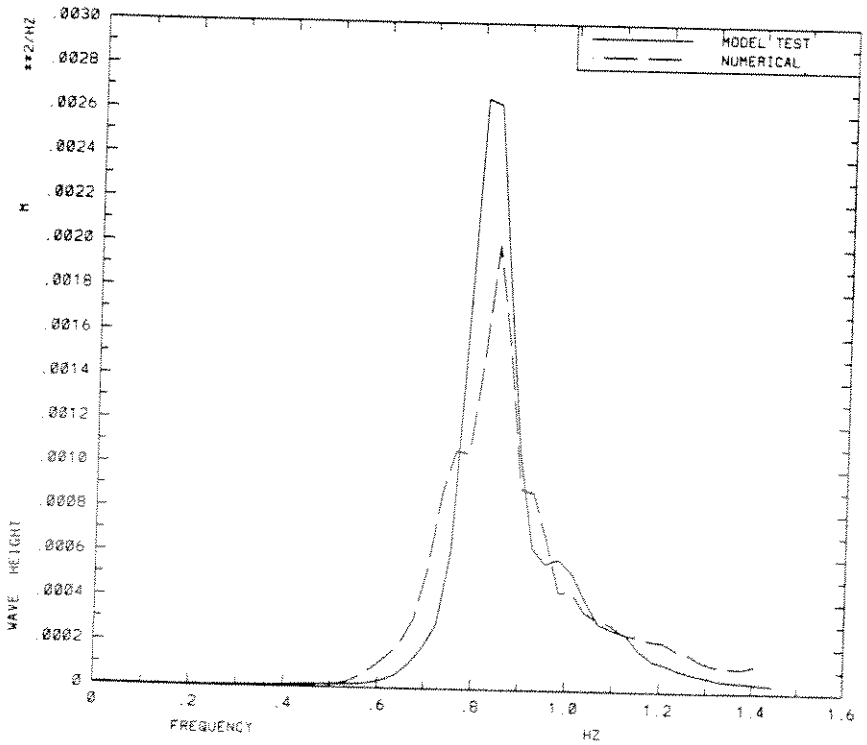

Fig. 31: Comparison of experimental and simulated wave spectra.
Wind speed u=3.9 m/s and sea state 2, H_s=0.087 m, T_p=1.19 s.

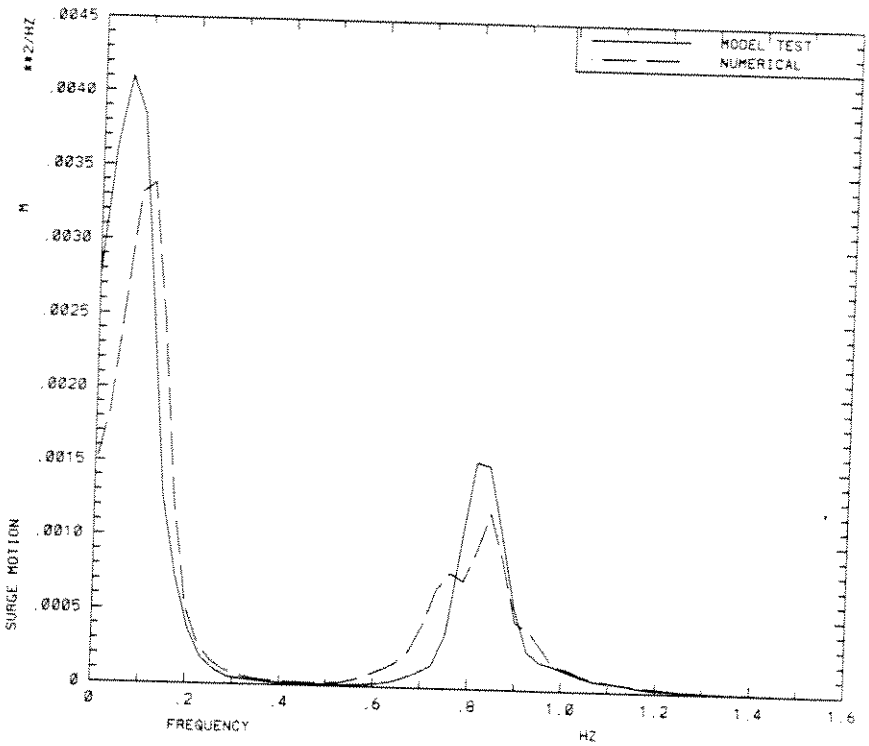

Fig. 32: Comparison of experimental and simulated surge motion spectra. Wind speed u=3.9 m/s and sea state 2, H_s=0.087 m, T_p=1.19 s.

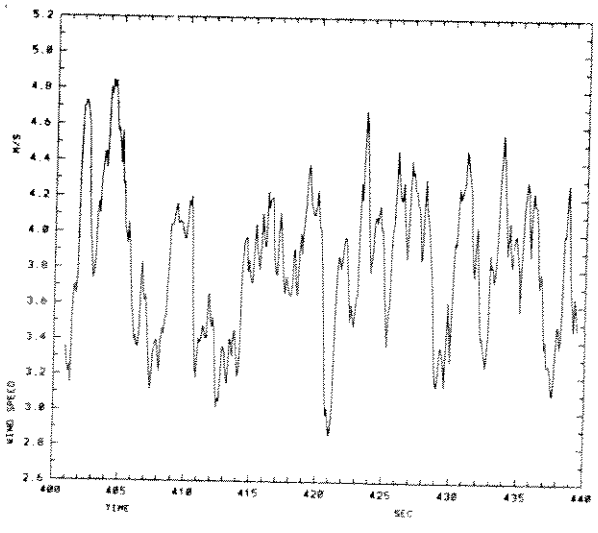

Fig. 33: Time period of experimental wind speed u=3.9 m/s.

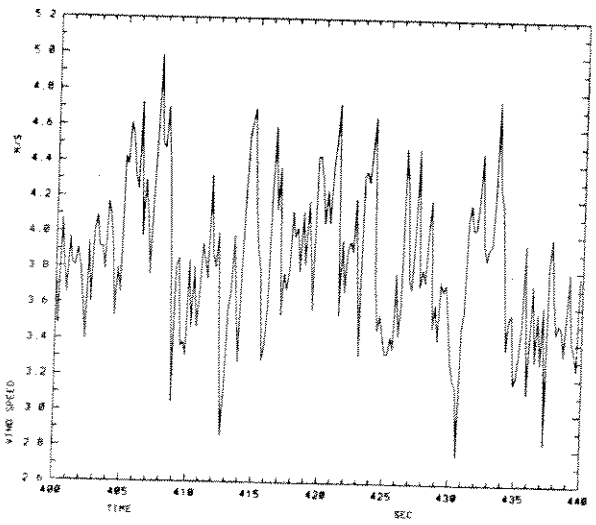

Fig. 34: Time period of simulated wind speed u=3.9 m/s.

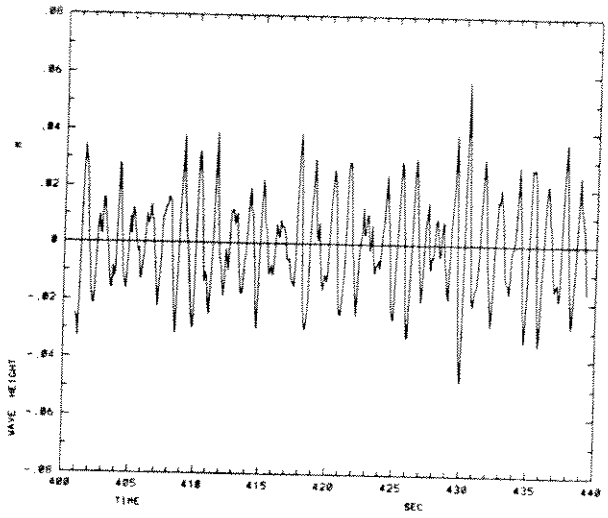

Fig. 35: Time period of experimental wave elevation sea state 2.

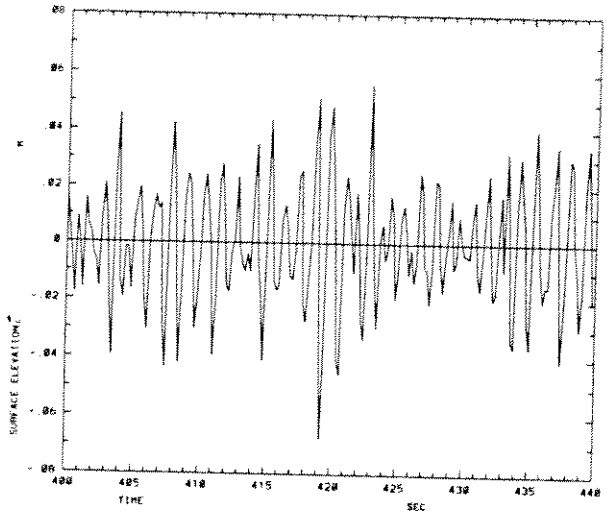

Fig. 36: Time period of simulated wave elevation sea state 2.

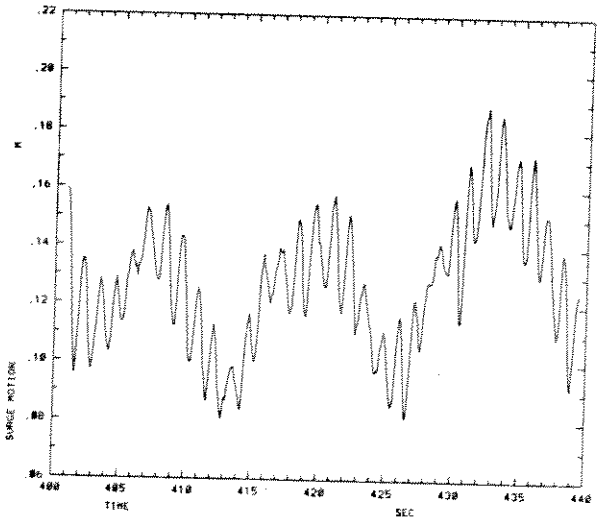

Fig. 37: Time period of experimental surge motion.

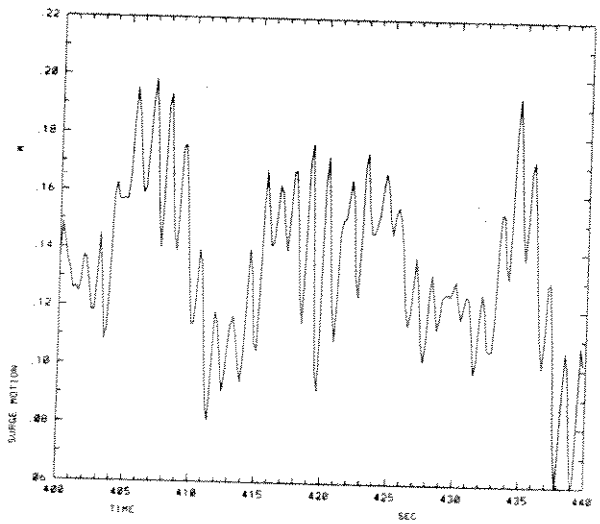

Fig. 38: Time period of simulated surge motion.

APPENDIX A

INPUT TO WADAM

```
SET TOLERANCE COORDINATES 0.1E-03
END
DEFINE POINT PT000 0. 0. 0.
PT001 .1905 0. 0.
PT002 0. .1905 0.
PT010 .1905 .1905 0.
PT012 .245 .1905 0.
PT013 .1905 .245 0.
PT100 0. 0. -.161
PT110 .1905 .1905 -.161
PT121 0. .214 -.161
PT122 0. .167 -.161
PT125 .167 0. -.161
PT126 .214 0. -.161
PT200 0. 0. -.196
PT210 .1905 .1905 -.196
PT211 .1905 .136 -.196
PT212 .245 .1905 -.196
PT213 .1905 .245 -.196
PT220 .214 .214 -.196
PT221 0. .214 -.196
PT222 0. .167 -.196
PT223 .167 .167 -.196
PT225 .167 0. -.196
PT226 .214 0. -.196
END
END
DEFINE SHAPE CYLINDER CYL1 PT010 PT210 .0545
END END
END
DEFINE SHAPE PLANE PL0 PT000 PT001 PT002
PL1 PT100 PT122 PT125
PL2 PT200 PT221 PT226
PLX1 PT226 PT220 PT126
PLX2 PT225 PT223 PT125
PLY1 PT221 PT220 PT121
PLY2 PT222 PT223 PT122
END END
 END
DEFINE POINT PT143 < SHAPE-INTERSECTION CYL1 PL1 PLX2 >
PT144 < SHAPE-INTERSECTION CYL1 PL1 PLX1 >
PT243 < SHAPE-INTERSECTION CYL1 PL2 PLX2 >
PT244 < SHAPE-INTERSECTION CYL1 PL2 PLX1 >
PT141 .160 .214 -.161
PT142 .160 .167 -.161
PT241 .160 .214 -.196
PT242 .160 .167 -.196
END
END
CHANGE POINT PT141 < SHAPE-INTERSECTION CYL1 PL1 PLY1 >
PT142 < SHAPE-INTERSECTION CYL1 PL1 PLY2 >
PT241 < SHAPE-INTERSECTION CYL1 PL2 PLY1 >
PT242 < SHAPE-INTERSECTION CYL1 PL2 PLY2 >
END
END
DEFINE POINT PT041 .141333 .214 0.
PT042 .141333 .167 0.
PT043 .167 .141333 0.
PT044 .214 .141333 0.
END
```

```
END
DEFINE ARC AR001 PT041 PT042 PT010 2
AR002 PT042 PT043 PT010 1
AR003 PT043 PT044 PT010 2
AR004 PT044 PT012 PT010 2
AR005 PT012 PT013 PT010 3
AR006 PT013 PT041 PT010 2
AR110 PT141 PT142 PT110 2
AR120 PT143 PT144 PT110 2
AR201 PT241 PT242 PT210 2
AR202 PT242 PT243 PT210 1
AR204 PT244 PT212 PT210 2
AR205 PT212 PT213 PT210 3
AR206 PT213 PT241 PT210 2
AR231 PT243 PT211 PT210 1
AR232 PT211 PT244 PT210 1
END
END
DEFINE LINE L102 PT121 PT122 2
L105 PT125 PT126 2
L111 PT141 PT121 4
L112 PT142 PT122 4
L113 PT143 PT125 4
L114 PT144 PT126 4
L202 PT221 PT222 2
L205 PT225 PT226 2
L211 PT241 PT221 4
L212 PT242 PT222 4
L213 PT243 PT225 4
L214 PT244 PT226 4
L221 PT211 PT210 2
L222 PT210 PT213 2
L0101 PT041 PT141 4
L0102 PT042 PT142 4
L0103 PT043 PT143 4
L0104 PT044 PT144 4
L1201 PT141 PT241 1
L1202 PT142 PT242 1
L1203 PT143 PT243 1
L1204 PT144 PT244 1
L1211 PT121 PT221 1
L1212 PT122 PT222 1
L1215 PT125 PT225 1
L1216 PT126 PT226 1
END
END
DEFINE SURFACE S102 AR110 L111 L102 L112
S103 AR120 L113 L105 L114
S202 AR201 L211 L202 L212
S203 AR232 NOT-MESH-CORNERS AR231 MESH-CORNERS L213 L205 L214
S211 L221 NOT-MESH-CORNERS L222 MESH-CORNERS AR206 NOT-MESH-CORNERS
 AR201 AR202 AR231
S212 L221 NOT-MESH-CORNERS L222 MESH-CORNERS AR205 NOT-MESH-CORNERS
 AR204 AR232
S0101 AR001 L0101 AR110 L0102
S0103 AR003 L0103 AR120 L0104
S0202 AR002 L0102 NOT-MESH-CORNERS L1202 MESH-CORNERS AR202 L1203
 NOT-MESH-CORNERS L0103
S0204 AR004 NOT-MESH-CORNERS AR005 AR006 MESH-CORNERS L0101
 NOT-MESH-CORNERS L1201 MESH-CORNERS AR206 NOT-MESH-CORNERS AR205 ,
```

```
 MESH-CORNERS L1204 NOT-MESH-CORNERS L0104
S1201 L111 L1201 L211 L1211
 S1202 L112 L1202 L212 L1212
S1203 L113 L1203 L213 L1215
S1204 L114 L1204 L214 L1216
END
END
SET NUMBEROF-ELEMENTS AR001 4 AR002 2 AR003 4 AR004 4 AR005 6 AR006
 AR110 4 AR120 4 AR201 4 AR202 2 AR204 4 AR205 6 AR206 4 AR231 2 AR
 2 END
END
SET NUMBEROF-ELEMENTS L102 4 L105 4 L111 8 L112 8 L113 8 L114 8 L20
 L205 4 L211 8 L212 8 L213 8 L214 8 L221 4 L222 4 L0101 10 L0102 10
 L0103 10 L0104 10 L1201 2 L1202 2 L1203 2 L1204 2 L1211 2 L1212 2
 L1215 2 L1216 2 END
END
SET ELEMENT-LENGTH-RATIO L0101 GIVEN-RELATIVE PT041 .25 .25 .5 1. 1
 1. 1. 1. 1. L0102 GIVEN-RELATIVE PT042 .25 .25 .5 1. 1. 1. 1. 1. 1
 L0103 GIVEN-RELATIVE PT043 .25 .25 .5 1. 1. 1. 1. 1. 1. 1. L0104
 GIVEN-RELATIVE PT044 .25 .25 .5 1. 1. 1. 1. 1. 1. 1. END
END
SET INSIDE S102 PT122 COORDINATES .1 .19 -.175
S103 PT125 COORDINATES .19 .1 -.175
S202 PT221 COORDINATES .1 .19 -.175
S203 PT225 COORDINATES .19 .1 -.175
S21& Z
S1201 PT221 COORDINATES .1 .19 -.175
S1202 PT122 COORDINATES .1 .19 -.175
S1203 PT125 COORDINATES .19 .1 -.175
S1204 PT226 COORDINATES .19 .1 -.175
S0103 PT043 COORDINATES .19 .19 0.
S0202 PT042 COORDINATES .19 .19 0.
S0204 PT044 COORDINATES .19 .19 0.
END
END
SET ELEMENT-TYPE SURFACE ALL-SURFACES-INCLUDED SHELL-4NODES END
END
PROPERTY LOAD 1 HYDRO-PRESSURE ALL-SURFACES-INCLUDED OUTSIDE
 OUTSIDE-SURFACE
END
END
MESH ALL
%%        PROCESSING SURFACE S102:
%%        COONS PATCH METHOD IS USED
%%           45 NODES
%%           32 BASIC ELEMENTS
%%        PROCESSING SURFACE S103:
%%        COONS PATCH METHOD IS USED
%%           45 NODES
%%           32 BASIC ELEMENTS
%%        PROCESSING SURFACE S202:
%%        COONS PATCH METHOD IS USED
%%           45 NODES
%%           32 BASIC ELEMENTS
%%        PROCESSING SURFACE S203:
%%        COONS PATCH METHOD IS USED
%%           45 NODES
%%           32 BASIC ELEMENTS
%%        PROCESSING SURFACE S211:
%%        ISOPARAMETRIC LAPLACE METHOD IS USED
```

```
%%            50 NODES
%%            39 BASIC ELEMENTS
%%          PROCESSING SURFACE S212:
%%          ISOPARAMETRIC LAPLACE METHOD IS USED
%%            50 NODES
%%            39 BASIC ELEMENTS
%%          PROCESSING SURFACE S0101:
%%          COONS PATCH METHOD IS USED
%%            55 NODES
%%            40 BASIC ELEMENTS
%%          PROCESSING SURFACE S0103:
%%          COONS PATCH METHOD IS USED
%%            55 NODES
%%            40 BASIC ELEMENTS
%%          PROCESSING SURFACE S0202:
%%          COONS PATCH METHOD IS USED
%%            39 NODES
%%            24 BASIC ELEMENTS
%%          PROCESSING SURFACE S0204:
%%          COONS PATCH METHOD IS USED
%%           195 NODES
%%           168 BASIC ELEMENTS
%%          PROCESSING SURFACE S1201:
%%          COONS PATCH METHOD IS USED
%%            27 NODES
%%            16 BASIC ELEMENTS
%%          PROCESSING SURFACE S1202:
%%          COONS PATCH METHOD IS USED
%%            27 NODES
%%            16 BASIC ELEMENTS
%%          PROCESSING SURFACE S1203:
%%          COONS PATCH METHOD IS USED
%%            27 NODES
%%            16 BASIC ELEMENTS
%%          PROCESSING SURFACE S1204:
%%          COONS PATCH METHOD IS USED
%%            27 NODES
%%            16 BASIC ELEMENTS
 WRITE 1
%%          RE-COMPUTING LOADCASE     1
%%            565 NODES WRITTEN
%%            542 BASIC ELEMENTS WRITTEN
%%      ** ELEMENT          1 HAS NO SECTION
%%      ** ELEMENT          2 HAS NO SECTION
%%      ** ELEMENT          3 HAS NO SECTION
%%      ** ELEMENT          4 HAS NO SECTION
%%      ** ELEMENT          5 HAS NO SECTION
%%      **     542 ELEMENTS HAVE NO SECTION
%%      ** ELEMENT          1 HAS NO MATERIAL
%%      ** ELEMENT          2 HAS NO MATERIAL
%%      ** ELEMENT          3 HAS NO MATERIAL
%%      ** ELEMENT          4 HAS NO MATERIAL
%%      ** ELEMENT          5 HAS NO MATERIAL
%%      **     542 ELEMENTS HAVE NO MATERIAL
%%              1 LOAD CASES WRITTEN
%%
%% CLOSED DATE: 18-FEB-1993  13:07:14
%%
```

2.7 SUMMARY OF MODEL PROPERTIES

ALL COORDINATES ARE GIVEN IN THE INPUT COORDINATE SYSTEM

THE RADII OF GYRATION AND CENTRIFUGAL MOMENTS OF THE MASS MATRIX
AND THE RESTORING COEFFICIENTS ARE GIVEN RELATIV TO THE MOTION REFERENCE P
(ORIGIN OF THE GLOBAL COORDINAT SYSTEM).

UNITS DATA:

ACCELERATION OF GRAVITY	G	= 9.81000E+00	[L/T*
WATER DENSITY	RHO	= 1.02500E+03	[M/L*

GEOMETRY DATA:

CHARACTERISTIC LENGTH	L	= 1.09000E-01	[L]
VERTICAL COORDINATE OF STILL WATER LINE	-ZLOC	= 0.00000E+00	[L]
NUMBER OF BASIC PANELS		= 542	
NUMBER OF SYMMETRY PLANES IN THE PANEL MODEL		= 2	
TOTAL NUMBER OF PANELS		= 2168	
DISPLACED VOLUMES OF THE PANEL MODEL	VOL 1	= 9.04350E-03	[L**3
	VOL 2	= 9.04349E-03	
	VOL 3	= 9.04349E-03	

MASS PROPERTIES AND STRUCTURAL DATA:

MASS OF THE STRUCTURE	M	= 6.58500E+00	[M]
WEIGHT OF THE STRUCTURE	M*G	= 6.45989E+01	[M*L/
CENTRE OF GRAVITY	XG	= 0.00000E+00	[L]
	YG	= 0.00000E+00	[L]
	ZG	= 6.70000E-02	[L]
ROLL RADIUS OF GYRATION	XRAD	= 2.42000E-01	[L]
PITCH RADIUS OF GYRATION	YRAD	= 2.43000E-01	[L]
YAW RADIUS OF GYRATION	ZRAD	= 2.35000E-01	[L]
ROLL-PITCH CENTRIFUGAL MOMENT	XYRAD	= 0.00000E+00	[L**2
ROLL-YAW CENTRIFUGAL MOMENT	XZRAD	= 0.00000E+00	[L**2
PITCH-YAW CENTRIFUGAL MOMENT	YZRAD	= 0.00000E+00	[L**2

HYDROSTATIC DATA:

DISPLACED VOLUME	VOL	= 9.04349E-03	[L**3
MASS OF DISPLACED VOLUME	RHO*VOL	= 9.26958E+00	[M]
WATER PLANE AREA	WPLA	= 3.68746E-02	[L**2

CENTRE OF BUOYANCY

	XCB	= 0.00000E+00	[L]
	YCB	= 0.00000E+00	[L]
	ZCB	=-1.14164E-01	[L]
TRANSVERSE METACENTRIC HEIGHT	GM4	= 1.40653E+01	[L]
LONGITUDINAL METACENTRIC HEIGHT	GM5	= 1.40653E+01	[L]
HEAVE-HEAVE RESTORING COEFFICIENT	C33	= 7.09078E+03	[M/T*
HEAVE-ROLL RESTORING COEFFICIENT	C34	= 0.00000E+00	[M*L/
HEAVE-PITCH RESTORING COEFFICIENT	C35	= 0.00000E+00	[M*L/
ROLL-ROLL RESTORING COEFFICIENT	C44	= 1.27902E+03	[M*L*
PITCH-PITCH RESTORING COEFFICIENT	C55	= 1.27902E+03	[M*L*
ROLL-PITCH RESTORING COEFFICIENT	C45	= 0.00000E+00	[M*L*

EQUILIBRIUM OF STATIC FORCES AND MOMENTS:

SUM OF TOTAL BUOYANCY AND GRAVITY FORCES	F3	= 2.63357E+01	[M*L/
STATIC MOMENT ABOUT THE X-AXIS	M1	= 0.00000E+00	[M*L*
STATIC MOMENT ABOUT THE Y-AXIS	M2	= 0.00000E+00	[M*L*
CORRESPONDING VERTICAL TRANSLATION		= 3.71408E-03	[L]
TRIM ANGLE IN ROLL	ALFAX	= 0.00000E+00	[DEG]
TRIM ANGLE IN PITCH	ALFAY	= 0.00000E+00	[DEG]

2.8 ENVIRONMENTAL DATA:

WATER DEPTH	= 1.69000E+00	[L]
NUMBER OF WAVE LENGTHS	= 14	
NUMBER OF HEADING ANGLES	= 1	

WAVE DESCRIPTION:

	WAVE LENGTH	WAVE NUMBER	WAVE PERIOD	WAVE ANG. FREQUENCY
1	1.00000E-01	6.28319E+01	2.53079E-01	2.48270E+01
2	1.40000E-01	4.48799E+01	2.99447E-01	2.09827E+01
3	1.90000E-01	3.30694E+01	3.48845E-01	1.80114E+01
4	2.50000E-01	2.51327E+01	4.00152E-01	1.57020E+01
5	3.90000E-01	1.61107E+01	4.99790E-01	1.25716E+01
6	5.60000E-01	1.12200E+01	5.98893E-01	1.04913E+01
7	7.70000E-01	8.15998E+00	7.02265E-01	8.94703E+00
8	1.00000E+00	6.28319E+00	8.00305E-01	7.85099E+00
9	1.26000E+00	4.98666E+00	8.98340E-01	6.99422E+00
10	1.56000E+00	4.02768E+00	9.99582E-01	6.28582E+00
11	1.89000E+00	3.32444E+00	1.10025E+00	5.71068E+00
12	2.25000E+00	2.79253E+00	1.20055E+00	5.23358E+00
13	2.64000E+00	2.37999E+00	1.30076E+00	4.83040E+00
14	3.06000E+00	2.05333E+00	1.40132E+00	4.48377E+00

HEADING ANGLES (ANGLE BETWEEN POS. X-AXIS AND DIRECTION OF WAVE PROPAGATION):

IN DEGREES	IN RADIANS

```
DEFINE
GENERAL TEXT 'TLP NEW CALCULATION'
 'WADAM DATA INTERFACE FILE FOR HYDROSTATIC CALCULATION'
 'PANEL MODEL ONLY'
END
END
DEFINE
GENERAL EXECUTION-DIRECTIVES ANALYSIS-TYPE GLOBAL-RESPONSE RESULT-FILES
 GLOBAL-RESPONSE GRIF END FIXED-FLOATING FLOATING YZ-XZ-PLANE YES
 DRIFT-FORCES YES SAVE-RESTART AUTO-SAVE-RESTART TOLERANCES
 COMPUTED-TOLERANCES 100.0 0.1 10.0 10.0 END END
CONSTANTS .109 1025.0 9.81 0. 0. 0. 0. 0.
ANALYSIS-MODELS MASS-MODEL GLOBAL-MASS-MATRIX USER-SPECIFIED 0. 0. .067
  .242 .243 .235 0. 0. 0. 6.585 SINK-SOURCE-MODEL 1 END
END
ENVIRONMENT WAVE-DIRECTION 0. END
WAVE-LENGTH 0.10 INFINITE 0.14 INFINITE 0.19 INFINITE 0.25 INFINITE
 0.39 INFINITE 0.56 INFINITE 0.77 INFINITE 1.00 INFINITE 1.26 INFINITE
 1.56 INFINITE 1.89 INFINITE 2.25 INFINITE 2.64 INFINITE 3.06 INFINITE
 END
%     ** NOTE: WADAM WILL USE THE OPTION FOR WAVE
%        APPROXIMATION GIVEN ON THE FIRST WAVE
%        LENGTH FOR ALL GIVEN WAVE LENGTHS
WATER-DEPTH 1.69
WAVE-AMPLITUDE 0.01 0.01 0.01 0.01 0.01 0.01 0.01 0.01 0.01 0.01 0.01
 0.01 0.01 0.01
END
END
DEFINE
GENERAL GLOBAL-MATRICES RESTORING-MATRIX 11 8.1 22 8.1 33 6720.0 44
 1280.0 55 1280.0 END END
END
END
;
 CLOSED DATE: 07-AUG-1992  15:28:23
```

APPENDIX B

EXAMPLE OF INPUT TO NV1427

```
BLWTL TLP
2 M/S WIND JONSWAP3-SPECTRUM SEA STATE 1 (Hs=0.060 m, Tz=0.767 s)
27.01.93
A1        1        0        0        1        1        0        0        1       25        0
A2     1.25   1025.0     1.69    9.810    0.242    0.243    2.350    0.000
A3    0.000    0.109   .00904     4.08 0.0000-0.0108-0.0108    6.585
A4     0.00     0.00
A5     1.71      0.0      1.0      0.0    150.0      1.0      9.0    30.00 20.0    0.0020
A6      5.0      0.0      1.0      0.0     60.0      1.0      8.0    1.300 20.000  0.100
      0.060    0.767    0.000    1.000    2.000    0.070    0.090    3.000
        0.0
      1.000
A9      1.0      2.0      0.0      1.0      0.0      0.0   3900.0      0.2 300.0 0.0020
        0.0      0.0      0.0      0.0      0.0      0.0
        0.0      0.0      0.0      0.0      0.0      0.0
B1     -1.0    +8.10      0.0      0.0      0.0      0.0      0.0
       -0.5    +4.05      0.0      0.0      0.0      0.0      0.0
       -0.1    +0.81      0.0      0.0      0.0      0.0      0.0
        0.0     0.00      0.0      0.0      0.0      0.0      0.0
        0.1    -0.81      0.0      0.0      0.0      0.0      0.0
        0.5    -4.05      0.0      0.0      0.0      0.0      0.0
        1.0    -8.10      0.0      0.0      0.0      0.0      0.0
B2     -1.0      0.0    +8.10      0.0      0.0      0.0      0.0
       -0.5      0.0    +4.05      0.0      0.0      0.0      0.0
       -0.1      0.0    +0.81      0.0      0.0      0.0      0.0
        0.0      0.0     0.00      0.0      0.0      0.0      0.0
        0.1      0.0    -0.81      0.0      0.0      0.0      0.0
        0.5      0.0    -4.05      0.0      0.0      0.0      0.0
        1.0      0.0    -8.10      0.0      0.0      0.0      0.0
B3   -0.20      0.0      0.0   +1344      0.0      0.0      0.0
     -0.10      0.0      0.0    +672      0.0      0.0      0.0
     -0.02      0.0      0.0  +134.4      0.0      0.0      0.0
      0.00      0.0      0.0     0.0      0.0      0.0      0.0
      0.02      0.0      0.0  -134.4      0.0      0.0      0.0
      0.10      0.0      0.0    -672      0.0      0.0      0.0
      0.20      0.0      0.0   -1344      0.0      0.0      0.0
B4   -0.12      0.0      0.0      0.0   +153.6      0.0      0.0
     -0.07      0.0      0.0      0.0    +89.6      0.0      0.0
     -0.03      0.0      0.0      0.0    +38.4      0.0      0.0
      0.0       0.0      0.0      0.0     0.00      0.0      0.0
      0.03      0.0      0.0      0.0    -38.4      0.0      0.0
      0.07      0.0      0.0      0.0    -89.6      0.0      0.0
      0.12      0.0      0.0      0.0   -153.6      0.0      0.0
B5   -0.12      0.0      0.0      0.0      0.0   +153.6      0.0
     -0.07      0.0      0.0      0.0      0.0    +89.6      0.0
     -0.03      0.0      0.0      0.0      0.0    +38.4      0.0
      0.00      0.0      0.0      0.0      0.0     0.00      0.0
      0.03      0.0      0.0      0.0      0.0    -38.4      0.0
      0.07      0.0      0.0      0.0      0.0    -89.6      0.0
      0.12      0.0      0.0      0.0      0.0   -153.6      0.0
B6    -0.3      0.0      0.0      0.0      0.0      0.0     0.21
      -0.2      0.0      0.0      0.0      0.0      0.0     0.14
      -0.1      0.0      0.0      0.0      0.0      0.0     0.07
       0.0      0.0      0.0      0.0      0.0      0.0      0.0
       0.1      0.0      0.0      0.0      0.0      0.0    -0.07
       0.2      0.0      0.0      0.0      0.0      0.0    -0.14
       0.3      0.0      0.0      0.0      0.0      0.0    -0.21
C1  4.4838
    4.8304
    5.2336
```

```
      5.7107
      6.2858
      6.9942
      7.8510
      8.9470
     10.4913
     12.5716
     15.7020
     18.0114
     20.9827
     24.8270
C2       0.0
C3   0.8062 0.0000 0.0000 0.0000 0.0000 0.0000
     0.0000 0.8062 0.0000 0.0000 0.0000 0.0000
     0.0000 0.0000 0.5882 0.0000 0.0000 0.0000
     0.0000 0.0000 0.0000 1.8572 0.0000 0.0000
     0.0000 0.0000 0.0000 0.0000 1.8553 0.0000
     0.0000 0.0000 0.0000 0.0000 0.0000 4.0082
C4   0.060  0.E+00 0.E+00 0.E+00 0.0000 0.E+00
     0.E+00 0.060  0.E+00 0.0000 0.E+00 0.E+00
     0.E+00 0.E+00 1.E-02 0.E+00 0.E+00 0.E+00
     0.E+00 0.0000 0.E+00 3.E-03 0.E+00 0.E+00
     0.0000 0.E+00 0.E+00 0.E+00 3.E-03 0.E+00
     0.E+00 0.E+00 0.E+00 0.E+00 0.E+00 3.E-03
C5   0.0028 0.0000 0.0000 0.0000 0.0000 0.0000
     0.0029 0.0000 0.0000 0.0000 0.0000 0.0000
     0.0030 0.0000 0.0000 0.0000 0.0000 0.0000
     0.0052 0.0000 0.0000 0.0000 0.0000 0.0000
     0.0212 0.0000 0.0000 0.0000 0.0000 0.0000
     0.1060 0.0000 0.0000 0.0000 0.0000 0.0000
     0.4013 0.0000 0.0000 0.0000 0.0000 0.0000
     0.8111 0.0000 0.0000 0.0000 0.0000 0.0000
     0.4500 0.0000 0.0000 0.0000 0.0000 0.0000
     0.5454 0.0000 0.0000 0.0000 0.0000 0.0000
     1.2789 0.0000 0.0000 0.0000 0.0000 0.0000
     1.0471 0.0000 0.0000 0.0000 0.0000 0.0000
     1.1594 0.0000 0.0000 0.0000 0.0000 0.0000
     1.0204 0.0000 0.0000 0.0000 0.0000 0.0000
C6   0.0067 0.0000 0.0198 0.0000 0.0000 0.0000
     0.0092 0.0000 0.0160 0.0000 0.0000 0.0000
     0.0128 0.0000 0.0115 0.0000 0.0000 0.0000
     0.0175 0.0000 0.0065 0.0000 0.0000 0.0000
     0.0236 0.0000 0.0007 0.0000 0.0000 0.0000
     0.0299 0.0000-0.0053 0.0000 0.0001 0.0000
     0.0315 0.0000-0.0089 0.0000 0.0002 0.0000
     0.0135 0.0000-0.0070 0.0000 0.0002 0.0000
    -0.0139 0.0000-0.0028 0.0000-0.0001 0.0000
     0.0379 0.0000 0.0014 0.0000 0.0003 0.0000
    -0.0177 0.0000-0.0004 0.0000-0.0001 0.0000
     0.0024 0.0000-0.0007 0.0000 0.0000 0.0000
    -0.0020 0.0000 0.0001 0.0000 0.0000 0.0000
     0.0106 0.0000 0.0020 0.0000 0.0000 0.0000
C7  -0.9003 0.0000 0.0006 0.0000-0.0005 0.0000
    -0.8408 0.0000 0.0005 0.0000-0.0006 0.0000
    -0.7682 0.0000 0.0004 0.0000-0.0008 0.0000
    -0.6779 0.0000 0.0002 0.0000-0.0009 0.0000
    -0.5644 0.0000 0.0000 0.0000-0.0010 0.0000
    -0.4214 0.0000 0.0005 0.0000-0.0011 0.0000
    -0.2514 0.0000 0.0024 0.0000-0.0010 0.0000
    -0.0480 0.0000 0.0029 0.0000-0.0005 0.0000
```

```
     0.2081 0.0000 0.0003 0.0000 0.0009 0.0000
     0.2809 0.0000 0.0011 0.0000 0.0021 0.0000
    -0.0201 0.0000 0.0003 0.0000 0.0000 0.0000
    -0.0646 0.0000-0.0002 0.0000-0.0005 0.0000
     0.0213 0.0000 0.0000 0.0000 0.0001 0.0000
    -0.0080 0.0000-0.0007 0.0000 0.0000 0.0000
D1   0.0     0.8324     0.0     0.0     0.0     0.0     0.0
     90.0    0.0000     0.0     0.0     0.0     0.0     0.0
     180.0 -0.8324      0.0     0.0     0.0     0.0     0.0
D2   0.0     0.0     0.0     0.0
D5   0.0     .1085 .00050 0.0000 0.0000 0.0000 0.000
Z
```